NOAA Technical Memorandum NWS SR-170

FIVE WSR-88D RADAR STUDIES

Peter L. Wolf
NWSO Tulsa, Oklahoma

Brian LaMarre
WSO Corpus Christi, Texas

Joseph C. Lowery and Richard D. Smith
NWSFO Memphis, Tennessee

Mark Richards and Tim Troutman
NWSO Nashville, Tennessee

Wayne Presnell and Jeff Borzilleri
WSO Daytona Beach, Florida

Scientific Services Division
Southern Region
Fort Worth, TX

October 1995

'ITED STATES
'ARTMENT OF COMMERCE
Ronald H. Brown, Secretary

National Oceanic and Atmospheric Administration
James Baker
Under Secretary and Administrator

National Weather Service
Elbert W. Friday
Assistant Administrator

TABLE OF CONTENTS

IMPORTANT LESSONS REGARDING TORNADO DEVELOPMENT AND DETECTION ILLUSTRATED BY THE DELAWARE COUNTY, OKLAHOMA, TORNADO

Peter L. Wolf
NWSO Tulsa, Oklahoma

1. Introduction

On May 26, 1995, a line of thunderstorms swept across much of eastern Oklahoma during the late morning and early afternoon hours. Some of the thunderstorms along the line became severe and produced large hail and high winds, as well as a brief tornado. Although atmospheric conditions were marginally favorable for thunderstorm rotation and brief tornado development (based on tornado forecast information described in Johns and Doswell 1992), the location of actual tornado development was atypical.

The case presented here challenges several conceptions that may still exist in the meteorological community regarding tornado development and detection. It illustrates that tornadoes do not always come from isolated storms, storms with a high Vertically Integrated Liquid (VIL) value, or storms with a strong mesocyclone. This case illustrates important points regarding radar detection that radar meteorologists need to know when similar events arise.

2. The Event

Environmental conditions were marginally supportive of thunderstorm rotation on May 26, 1995. The air mass was moderately unstable across northeastern Oklahoma, with greater instability existing over southeastern Oklahoma. Area wind profilers and the WSR-88D VAD Wind Profile (not shown) indicated nearly uniform southerly to southwesterly flow with weak speed shear. The wind did veer with height in the lowest 1 km above ground level (AGL), but wind speeds in this layer were generally 20 kt or less.

At 11 a.m. CDT, the Inola, Oklahoma, WSR-88D radar indicated a nearly solid line of strong thunderstorms over east-central Oklahoma (not shown). The thunderstorms were not severe, but they were producing heavy rain and gusty winds. During the next hour, the northern portion of the line became cellular, while the southern portion remained solid and intensified (Fig. 1a). The individual storms over northeastern Oklahoma did not produce high winds or hail, while the southernmost storms in the line did.

The southernmost storms shown on Figs. 1a and 1b appeared to be the ones most favorable to become tornadic because of stronger updrafts (as implied by much higher VILs), greater instability, and better inflow from the south. Moderate mid-level rotation was indicated in the southern storms.

The southernmost storms were severe but never became tornadic. The one tornado reported on May 26 was produced by one of the low VIL storms over northeastern Oklahoma. Even though the tornadic storm had a VIL value less than 30 kg/m^2 (Fig. 1b), a tornado warning was issued

for southeastern Delaware County based on storm-relative velocity imagery (Fig. 1e) and the mesocyclone indicated by the mesocyclone detection algorithm in prior volume scans. The tornado touched down about 5 min after the warning was issued.

Figures 1c and 1d are the 0.5-deg and 2.4-deg storm-relative velocity images available 20 to 25 min before the tornado developed (1645 UTC). Figures 1e and 1f are similar to 1c and 1d, except for the 1703 UTC volume scan which was completed a few minutes prior to tornado development. The 0.5-deg images show the storm-relative velocity pattern for the Delaware County storm at about 4,000 ft AGL, while the 2.4-deg images show the pattern for the storm at 14,000 ft AGL (adjusting mean-sea-level heights given by the radar to AGL heights).

At 2.4 deg, the WSR-88D imagery showed a decrease in mid-level rotational velocity during the 20-min period prior to tornado development, with divergence more evident than rotation near the time of tornado development. For the volume scan prior to tornado development (1703 UTC), a mesocyclone indicated during the two previous volume scans by the WSR-88D mesocyclone detection algorithm was no longer indicated.

At 0.5 deg, convergence evolved into rotation during the 20-min period prior to tornado development. A gate-to-gate rotational velocity greater than 35 kt (at least 22 kt outbound and at least 50 kt inbound) was evident just prior to tornado development. Two volume scans later, this "tornadic vortex signature" (TVS) fell apart, leaving a weak, broad rotation. The WSR-88D TVS algorithm never alarmed, even though the thunderstorm was just 40 mi from the radar site, and the rotation met TVS criteria (inbound velocity plus outbound velocity totalling 70 kt or more). The TVS algorithm may not have alarmed because no mesocyclone was indicated by the time the rotational velocity at 0.5 deg met TVS criteria.

Figures 1e and 1f show an interesting aspect of the tornadic rotation. A complex pattern is seen at 2.4 deg (Fig. 1f), with a gate-to-gate divergence signature directly above the TVS seen on the 0.5-deg elevation angle (Fig. 1e). The tornado appeared to be confined to the lowest 10,000 ft of the storm.

Around 12:10 p.m. CDT, a small tornado touched down briefly over southeastern Delaware County about a mile southwest of the town of Colcord. Trees and power lines were downed with rotation evident in the damage pattern. Several outbuildings were also damaged by the tornado. Fortunately, the tornado dissipated before reaching Colcord.

3. Discussion

This event reinforces several important points regarding tornado detection with the WSR-88D, especially with respect to tornadoes that are not generated by large isolated supercell thunderstorms. The information presented below may be useful to other radar meteorologists during future severe thunderstorm events.

As this case illustrates, tornadoes do not always come from the storms with high VILs. The Delaware County storm had a VIL of only 25 to 30 kg/m^2. A similar occurrence was noted during an April 1995 event when a high-precipitation (HP) supercell over Okay, Oklahoma, with

a VIL in the 30s produced a strong tornado. Despite the relatively low VILs, both storms exhibited substantial overhang. While tornadic storms often have high VILs, there is no apparent correlation between VIL values and tornado development, because high VILs are often not associated with tornadoes.

Tornado formation within a solid thunderstorm line is rare. However, tornado potential can increase when a solid line breaks up into individual cells, or possibly into supercells if environmental conditions are favorable. Even if supercells do not form, non-supercellular tornadoes, such as "gustnadoes" and "landspouts" (Doswell and Burgess 1993, Burgess et al. 1993), may develop from cells that were once part of a solid line.

While tornadic thunderstorms often exhibit deep, strong rotation prior to and during tornado development, this will not always be the case. In the Delaware County thunderstorm, moderate rotation existed below 15,000 ft AGL for several volume scans prior to tornado formation; but the rotation weakened during tornado formation to the point where a mesocyclone could not be identified by the WSR-88D mesocyclone detection algorithm. This loss of mesocyclone detection by the algorithm provided a false indication that the threat of tornado development was diminishing.

As illustrated by this storm and several others across eastern Oklahoma in 1995, tornado development can occur rapidly, often in less than 15 min after the initial indication of low-level rotation. In the Delaware County example, low-level rotation developed, increased to the point where a TVS was observed in the storm-relative velocity product and decreased substantially—all within a 20- to 30-min period.

The Delaware County case illustrates important points to remember regarding tornado detection:

(1) Avoid focusing on any one storm or group of storms. For the May 26, 1995, event, the most severe storms appeared to be on the southern portion of a line. However, the tornado developed from a storm that did not appear to be severe on the northern portion of the line. Focusing solely on the southern storms could have led to no warning for the Delaware County tornado.

(2) There is no known correlation between VIL and tornadoes. A low VIL value does not eliminate the chance of a tornado. Likewise, a high VIL value does not ensure tornado development. Despite having a low VIL, the Delaware County thunderstorm exhibited favorable structure, with substantial overhang noted. Storm structure may be more important than the VIL value.

(3) Due to radar sampling limitations (as described in the *WSR-88D Operator's Guide to Mesocyclone Recognition and Diagnosis*, pages 44-55, available from the WSR-88D Operational Support Facility in Norman, Oklahoma), the WSR-88D algorithms will not be able to detect all mesocyclones and tornado vortex signatures, as the Delaware County tornado case illustrated. Do not depend solely on the algorithms to locate all severe weather activity.

4. Acknowledgments

The author wishes to thank Steve Amburn (Science and Operations Officer) and Greg Patrick of WSFO Tulsa for their reviews of the text.

5. References

Burgess, D.W., R.J. Donaldson, Jr., and P.R. Desrochers 1993: Tornado Detection and Warning by Radar. *The Tornado: Its Structure, Dynamics, Prediction, and Hazards.* American Geophysical Union, Washington DC, 203-221.

Doswell, C.A. and D.W. Burgess 1993: Tornadoes and Tornadic Storms: A Review of Conceptual Models. *The Tornado: Its Structure, Dynamics, Prediction, and Hazards.* American Geophysical Union, Washington DC, 161-172.

Johns, R.H. and C.A. Doswell III 1992: Severe Local Storms Forecasting. *Bull. Amer. Meteor. Soc.,* 7, 588-612.

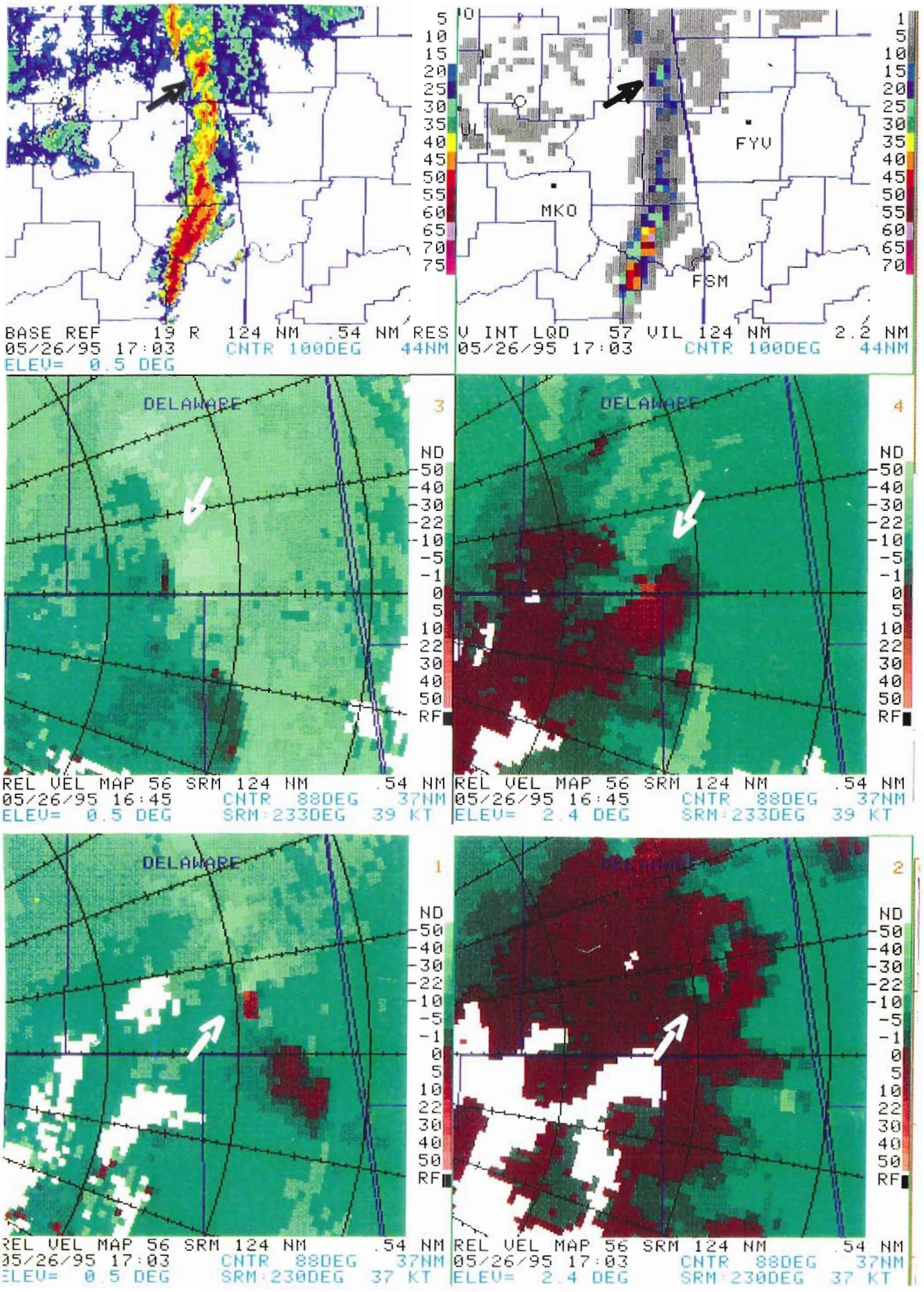

Fig. 1. WSR-88D products for May 26, 1995.
See text for explanation.

A MULTI-SCALE EXAMINATION OF SEVERE THUNDERSTORM DEVELOPMENT OVER NORTH CENTRAL TEXAS

Brian LaMarre
National Weather Service Office
Corpus Christi, Texas

1. Introduction

On July 24, 1995, an isolated area of severe thunderstorms developed over North-Central Texas and produced a variety of severe weather, including 22 reports of wind damage, 13 reports of hail up to softball size, and one reported tornado.

The thunderstorm complex developed just to the north of San Angelo, rapidly intensified as it moved northeastward toward Abilene, and dissipated west of the Dallas/Fort Worth metropolitan area. This study analyzes the synoptic and mesoscale environment on July 24 over north-central Texas, with an emphasis on the role of thermodynamics and kinematics. Detailed meteorological fields derived from the Eta model and generated through PC-GRIDDS (Meier 1993) are presented. In addition, WSR-88D base reflectivity (R) and storm relative motion (SRM) data are studied.

2. Mesoanalysis and Synoptic Discussion

Gridded data products were used to depict significant thermodynamic and kinematic features of the pre-storm environment. Specific fields were chosen for examination: 850 mb equivalent potential temperature (Theta-e) and dew-point, 850 and 500 mb thermal and velocity fields, as well as divergence. Additionally, the vertical velocity and lifted index analyses were used to depict an overall environment of atmospheric instability which, in turn, revealed a gradient leading to cell propagation. In the study of convective development, these meteorological fields and parameters are used with success when specific features, established through past studies and forecaster experience, exist across a defined area.

The 12-hr forecast run from the Eta model, 25/0000 UTC, revealed a high potential for convection over North-Central Texas. Between 24/2000 UTC and 25/0000 UTC, cells developed rapidly. A surface analysis (not shown) depicted a nearly stationary boundary extending from southwest Arkansas westward across North-Central Texas. The surface boundary intersected a dry line located to the southwest of Abilene.

Between 24/1200 UTC and 25/0000 UTC, a gradient developed in the 850 mb Theta-e field over north-central Texas, as evident in the 12-hr Eta model forecast shown in Fig. 1a. A significant increase in low-level moisture was also evident at 850 mb during the same period (Fig. 1b).

Forecast temperatures at 850 mb (Fig. 2a) depict a thermal trough from central Missouri, extending southwestward to North Texas. A thermal ridge lies along a line from North-Central

Texas to central Alabama. In contrast, the 500 mb temperature field (Fig. 2b) reveals a thermal trough from western Kansas southward to far West Texas.

The low and mid-level synoptic wind field forecasts at 850 and 500 mb (Fig. 3) show a southerly low-level jet at 850 mb, advecting the warm and moist air northward into North-Central Texas. At 500 mb, the wind veers to a westerly component over the area of interest. The directional shear between the two levels, combined with the low-level thermodynamic forcing, represents a possible explanation for the tornadic development within the convective complex.

Another interesting feature can be seen in Fig. 4. Given developments over North-Central Texas, low-level convergence and mid-level divergence of the total wind (the addition of the geostrophic and ageostrophic wind) would be expected. The forecast divergence field reveals this scenario. At 850 mb, convergence (dashed) exists across North-Central Texas, while at 500 mb divergence (solid) is seen from the western portions of Texas northeastward across North-Central Texas.

The forecast 700 mb vertical velocity (Fig. 5) and surface-based lifted index (Fig. 6), both valid at 25/0000 UTC, show areas of maximum vertical motion and instability to the northeast of where the convection developed. In this study, the gradients of instability associated with these two particular synoptic fields exist in direct correlation with storm motion which, as the gradient suggests, is oriented from southwest to northeast.

3. Doppler Radar Interpretation

WSR-88D radar imagery from NWSO Midland was used to identify stages of convective development. Fig. 7 shows base reflectivity during the time period of 24/2139 UTC to 24/2244 UTC. SRM is also shown at 24/2244 UTC. SRM data is useful in detecting areas of rotation, shear, and divergence in thunderstorm cells by subtracting the average motion of all identified storms (Klazura 1993).

The reflectivity field at 24/2139 UTC indicated thunderstorm development to the north-northeast of Robert Lee. Between 24/2208 and 24/2244 UTC, the storm intensified and maintained maximum reflectivity values of 55-60 dBZ during its track toward Abilene. A second cell developed just to the west of Sweetwater and merged with the Abilene storm. At 24/2244 UTC, the now multi-cellular complex developed a weak rotation in the cell to the southwest of Abilene, as indicated by the SRM data. The storm propagated northeastward toward Abilene producing a tornado less than 30 min later at 24/2312 UTC.

The reflectivity field at 24/2331 UTC (not shown) revealed stages of weakening, or possible collapse, in the cell over Abilene, resulting in several reports of wind and hail damage, including a 63-mph wind gust at the WSO in Abilene at 24/2328 UTC. The cell remained intense with maximum reflectivity values of 65-70 dBZ and was also responsible for widespread wind and hail damage, including 4-in diameter hail (softball size) across the cities of Eolian (25/0030) and South Bend (25/0120), southwest and northwest of Mineral Wells, respectively.

4. Summary

This study analyzed the synoptic and mesoscale features leading to the development and propagation of thunderstorms across North-Central Texas on July 24, 1995. Forecast analyses from the Eta model revealed thermodynamic and kinematic forcing processes leading to severe thunderstorm initiation.

Storms developed rapidly across a nearly stationary surface boundary beneath favorable 850 mb Theta-e and dew-point gradients, along with the intersection of the low and mid-level thermal axes. Sufficient instability and directional shear were also present in the pre-storm environment. The storm cells developed north of San Angelo, intensified as the complex moved toward Abilene, and dissipated near Mineral Wells.

Doppler reflectivity data were used to study the stages of development, propagation, and dissipation. SRM showed rotation in the cell near Abilene, possibly associated with the tornado reported in that vicinity.

5. Acknowledgments

I would like to thank Greg Jackson (NWSO Midland) for providing the WSR-88D products used in this study and for his detailed interpretation of the data. The Scientific Services Division at NWS Southern Region Headquarters provided final review and editing.

6. References

Klazura, G.E., and D.A. Imy, 1993: A Description of the Initial Set of Analysis Products Available from the NEXRAD WSR-88D System. *Bull. Amer. Met. Soc.*, 74, 1293-1311.

Meier, K., 1993: *PC-GRIDDS: A User's Manual.* National Weather Service, Western Region Headquarters, Salt Lake City, Utah. 102 pp.

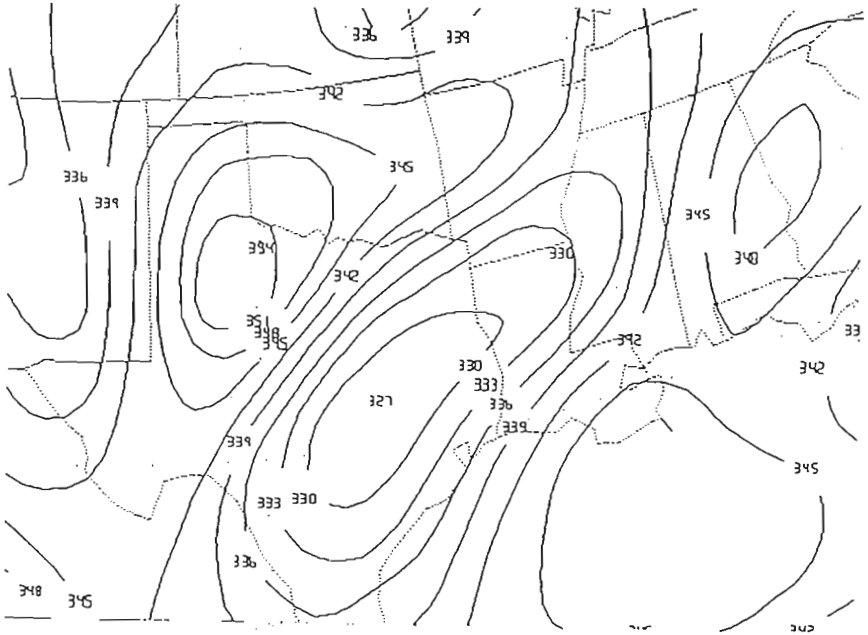

Figure 1a. 850 mb Theta-e analysis (°K) valid 0000 UTC 25 July 1995 from the Twelve-hour Eta forecast.

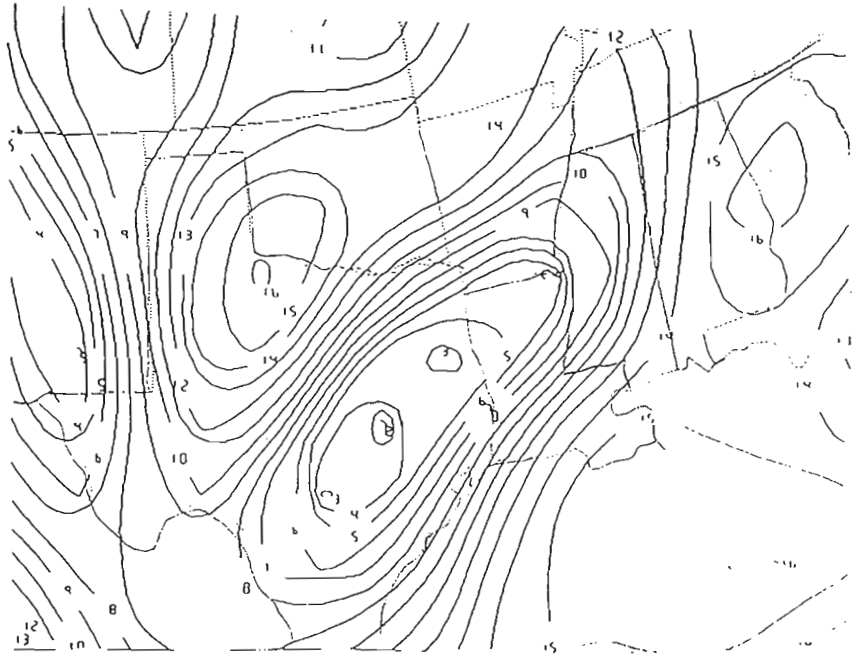

Figure 1b. 850 mb Dew-point analysis (°C) valid 0000 UTC 25 July 1995 from the Twelve-hour Eta forecast.

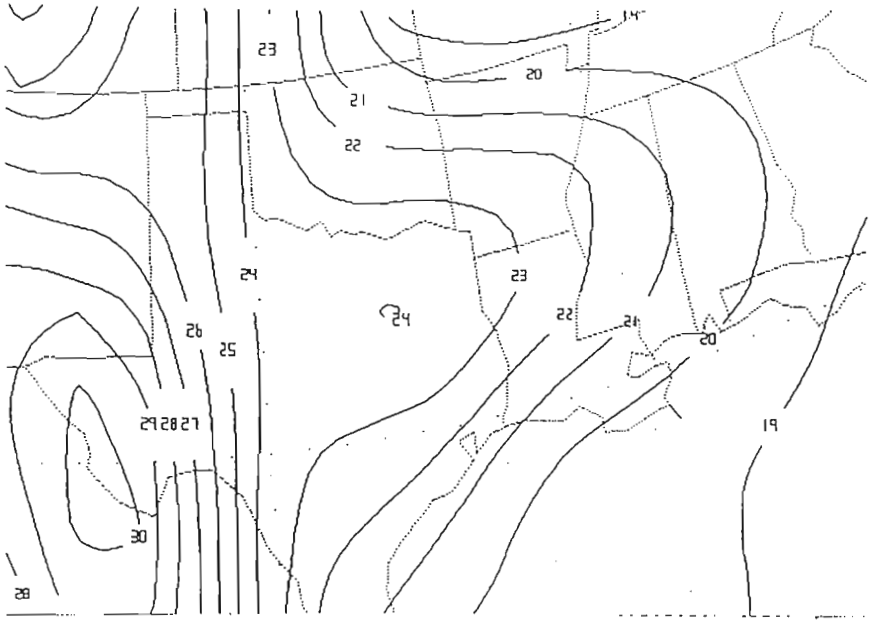

Figure 2a. 850 mb Temperature analysis (°C) valid 0000 UTC 25 July 1995 from the Twelve-hour Eta forecast.

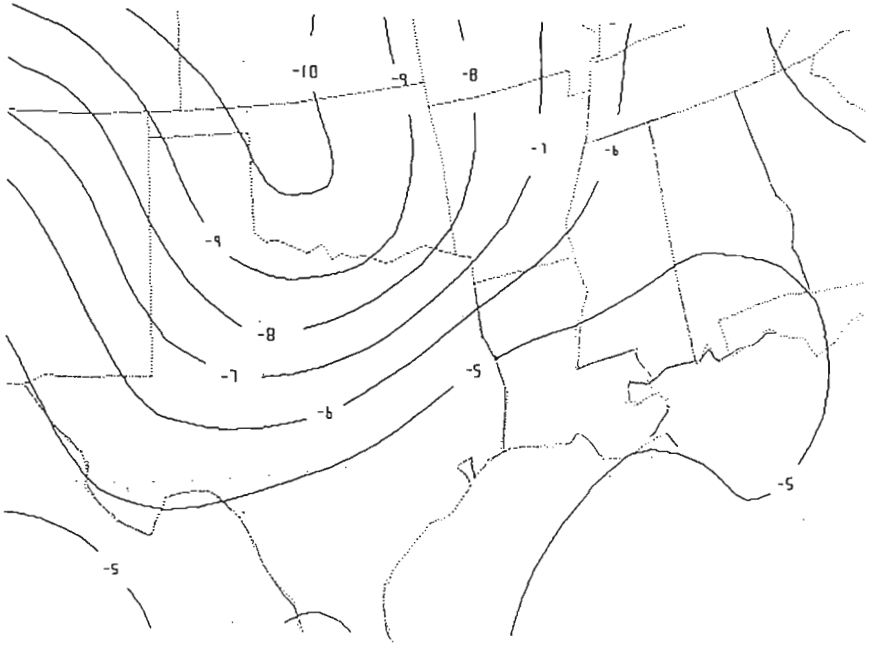

Figure 2b. 500 mb Temperature analysis (°C) valid 0000 UTC 25 July 1995 from the Twelve-hour Eta forecast.

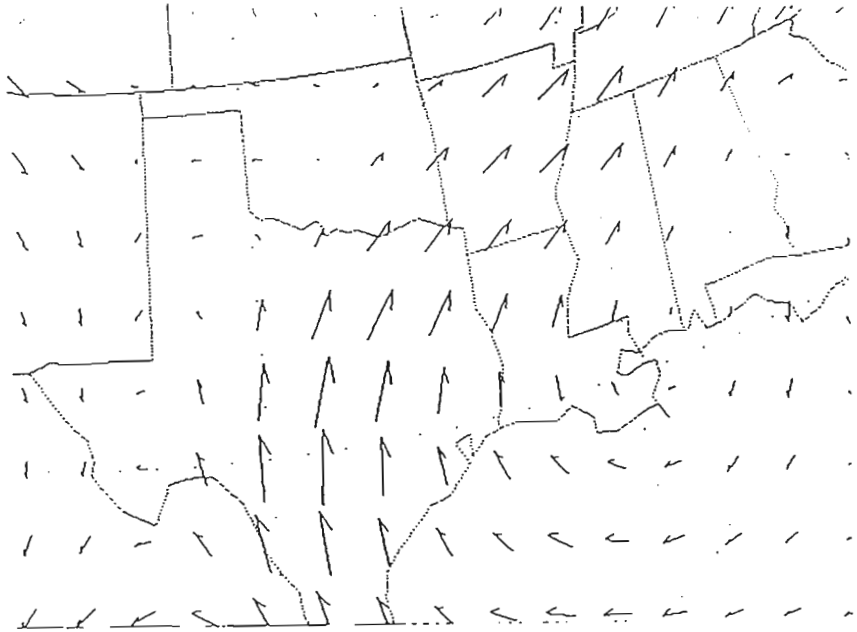

Figure 3a. 850 mb Wind field (magnitude depicted by the length of the vector) valid 0000 UTC 25 July 1995 from the Twelve-hour Eta forecast.

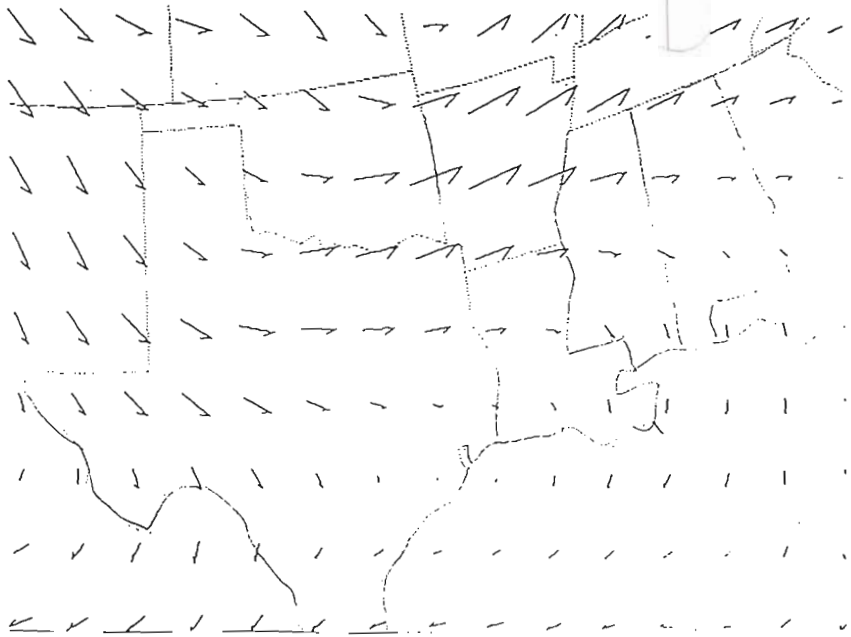

Figure 3b. 500 mb Wind field (magnitude depicted by the length of the vector) valid 0000 UTC 25 July 1995 from the Twelve-hour Eta forecast.

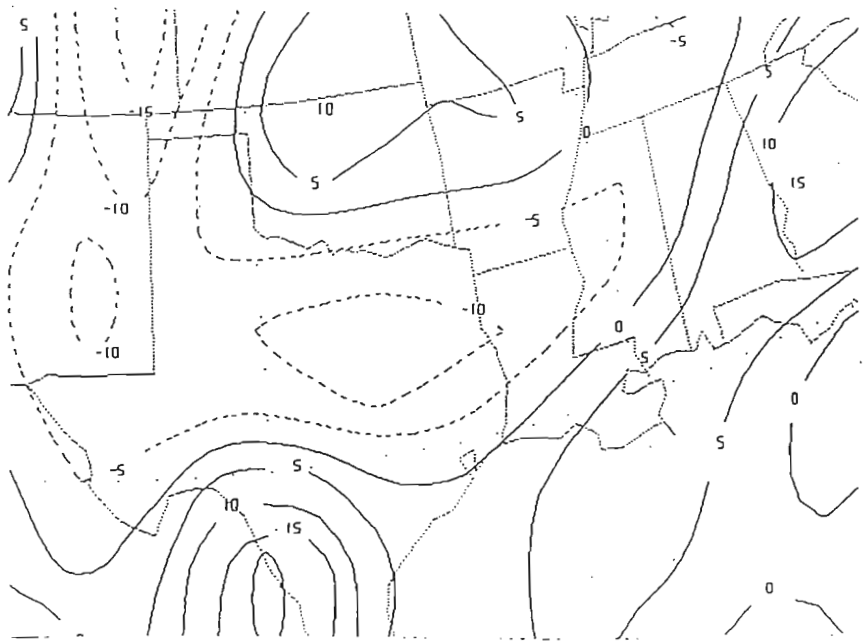

Figure 4a. 850 mb Divergence field, dashed (negative) values denote convergence of the total wind, valid 0000 UTC 25 July 1995 from the Twelve-hour Eta forecast.

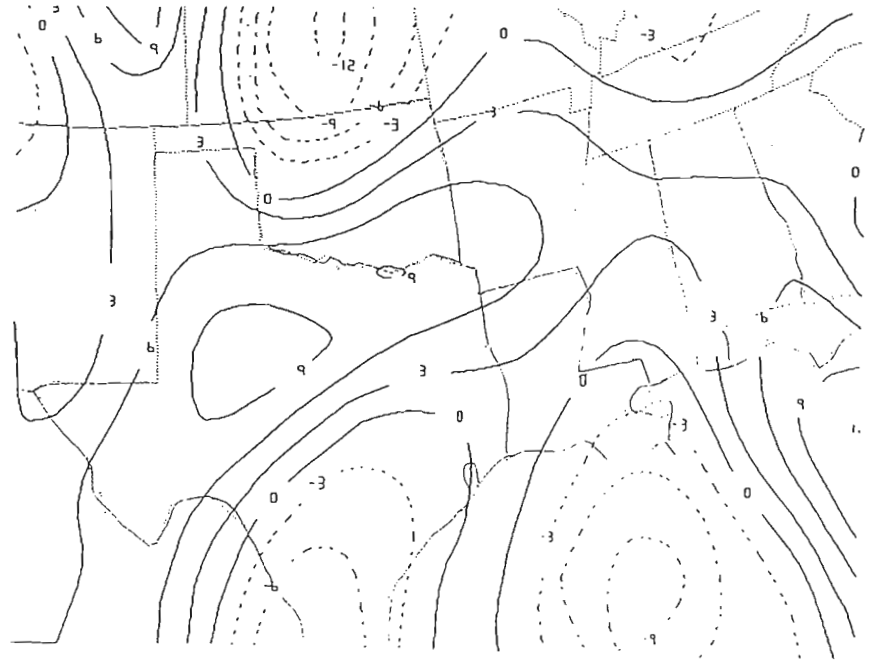

Figure 4b. 500 mb Divergence field, solid (positive) values denote divergence of the total wind, valid 0000 UTC 25 July 1995 from the Twelve-hour Eta forecast.

Figure 5. 700 mb Vertical Velocity field (microbars/second), dashed (negative) values depict upward vertical motion, valid 0000 UTC 25 July 1995 from the Twelve-hour Eta forecast.

Figure 6. Surface-based Lifted Index (°C) analysis valid 0000 UTC 25 July 1995 from the Twelve-hour Eta forecast.

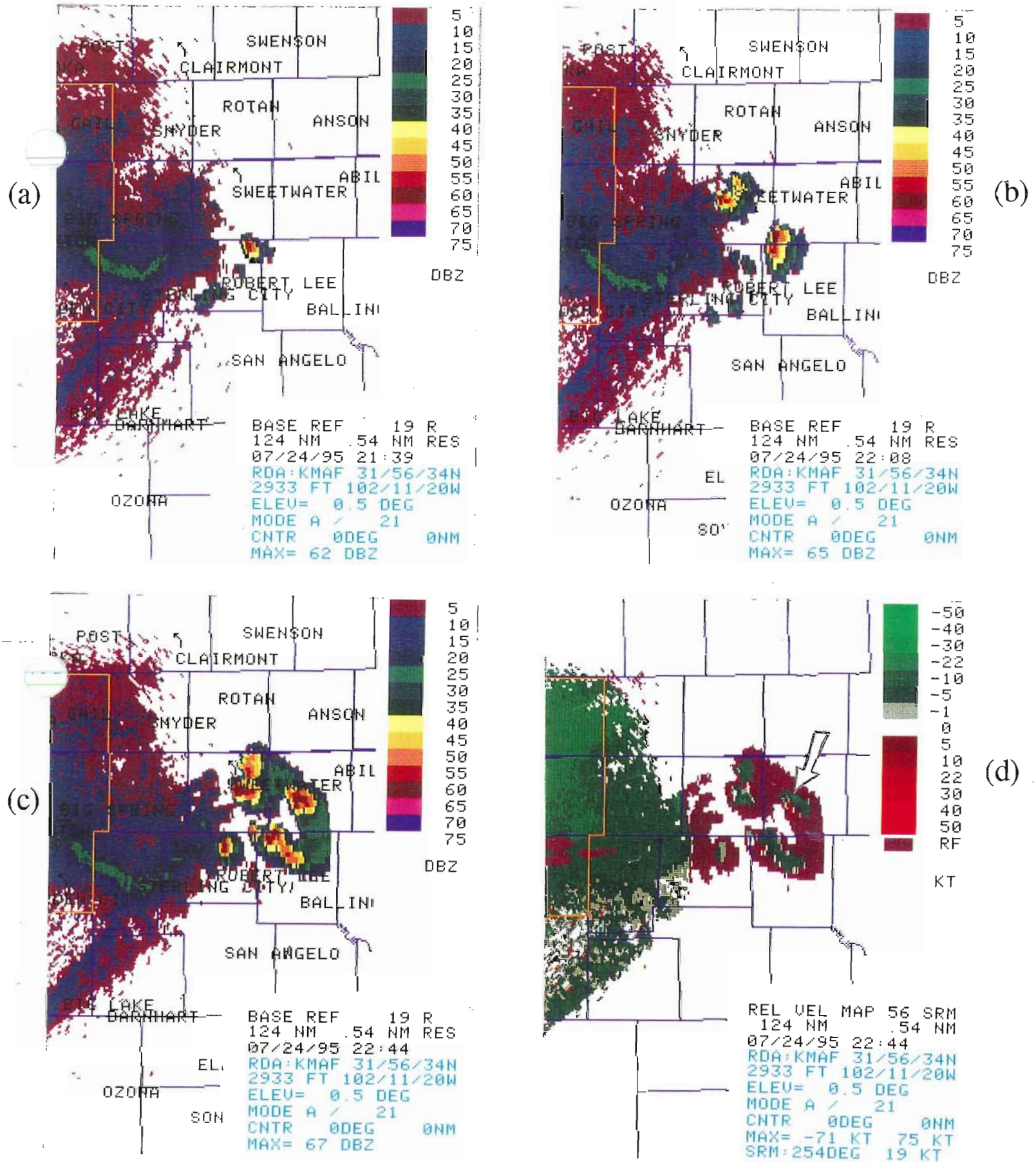

Fig. 7. Midland WSR-88D products showing evolution of July 24, 1995, storm. (a) - (c), 0.5 deg base reflectivity; (d) 0.5 deg storm relative velocity. See text for details.

METEOROLOGICAL AND OPERATIONAL ASPECTS OF THE GERMANTOWN TORNADO — NOVEMBER 27, 1994

Joseph C. Lowery and Richard D. Smith
NWSFO Memphis Tennessee

1. Introduction

A strong tornado roared through a section of Germantown, Tennessee, on Sunday, November 27, 1994. The tornado touched down in this Memphis suburb around 3:20 p.m. CST. Travelling northeast through Germantown, the tornado killed three persons, injured 22, and caused $60 million in property damage as it ripped through an upscale neighborhood. The tornado was on the ground for approximately 11 mi (Fig. 1) and was rated an F3 on the Fujita intensity scale. This paper will focus on the synoptic and mesoscale features associated with the tornado, and look at how NWSFO Memphis handled the event.

The Germantown tornado was one of a series of tornadoes that affected parts of east Arkansas and west Tennessee that Sunday afternoon. During a period of one-and-a-half hours, tornadoes struck West Memphis, Arkansas, and parts of Tipton, Crockett, and Weakley Counties in west Tennessee (Fig. 2). Meteorological conditions associated with the Germantown tornado were classic in many ways. The tornado occurred in late November, a time of year climatologically favored for tornadoes in the mid-South (Gaffin and Smith 1995). In addition, the tornado struck at mid afternoon, the diurnal peak for strong tornadoes in west Tennessee.

2. Synoptic Scale Features

Synoptic scale features preceding the Germantown tornado pointed to a significant potential for tornado and severe thunderstorm development on November 27. The combination of strong dynamics and thermodynamics made for a volatile situation that day. At 2100 UTC, shortly before the tornado, a surface analysis showed a 985 mb low centered over northern Iowa (Fig. 3). A cold front stretched southward from the low into central Arkansas. A surface trough (dry line) was located over eastern Arkansas ahead of the cold front. Across west Tennessee winds were strong and gusty from the south, temperatures climbed into the 70s, and dewpoints were in the middle 60s. Just west of the approaching dry line, temperatures remained in the 70s; but dewpoints fell into the 40s.

At Memphis International Airport 12 mi west of Germantown, the temperature peaked at 74 F at 1900 UTC. Strong south winds buffeted west Tennessee during the day, with gusts as high as 40 mph recorded in the hours immediately preceding the tornado. It is important to note that while winds over eastern Arkansas turned to a southwesterly direction, winds at the Memphis observation site remained from the south between 180 and 200 deg. This would play a significant role in maintaining high storm-relative helicity across southwest Tennessee.

The 1200 UTC 850 mb data on the 27th showed a closed low over southeast Nebraska with a 50- to 60-kt low-level jet pushing into western Arkansas from the Gulf of Mexico (Fig. 4a). An axis of 12 C dewpoints extended from northern Louisiana into eastern Arkansas, and a thermal

ridge existed to the west of the moisture axis, with 15 C temperatures extending from East Texas into western Arkansas (Fig. 4b). Strong southwest winds were advecting this warm air toward the area of greatest moisture— a favorable ingredient for the development of severe storms.

Further aloft at 1200 UTC, dry air was being advected into west Tennessee at 700 mb, and mean relative humidities of less than 50 percent were moving toward west Tennessee (Fig. 5a). Even drier air was poised to the southwest over Texas and Louisiana. At 500 mb (Fig. 5b), a deepening negatively tilted trough was apparent—a common feature associated with severe weather in the mid-South. At 200 mb a strong jet stream (120 to 130 kt) extended from northern Texas into Ohio, and divergence was also evident at that level from the Southern Plains into Tennessee (not shown).

3. Soundings and Hodographs

Figure 6a shows the SHARP (Hart and Korotky 1991) analysis of the 1200 UTC sounding from Little Rock. At the time of the sounding, Little Rock was east of the approaching cold front and surface trough. The sounding indicated a convectively unstable and moist, but capped, air mass with a 500 mb Lifted Index of -6 C and a CAPE of 1488 J/kg.

The modified sounding (Fig. 6b) approximates conditions at the time of the Germantown tornado. Temperature and dewpoint data used to modify the sounding were chosen from hourly surface observations, upper air data from the subsequent 0000 UTC sounding, and NGM forecast data valid at 1800 UTC on the 27th. The SHARP program calculated the following parameters from the modified sounding for the time of the tornado:

500 mb Lifted Index	-6 C
300 mb Lifted Index	-4 C
SWEAT Index	380
K Index	26
Total Totals	49
CAPE	1787 J/Kg
Cap Strength	0 C
Bulk Richardson Number	11
Energy-Helicity Index	3.9
Max Upward Vertical Velocity	60 m/s
Wet Bulb Zero Height	9417 feet

In addition, a hodograph (Fig. 6c) representative of conditions just prior to the tornado was produced using VAD wind profile data (not shown) from the Memphis WSR-88D, 17 mi north-northwest of Germantown. Surface observations from Memphis International Airport were also used, as was the actual storm movement (237 deg at 44 kt). Using observed storm motion, SHARP calculated a 0-2 km storm-relative helicity of 348 m^2/s^2, with a mean storm inflow of 137 deg at 16 kt.

Comparing CAPE versus storm-relative helicity, it can be seen that conditions were ripe for the formation of a strong tornado. The modified sounding yielded a CAPE of 1787 J/kg, a 0-2 km storm-relative helicity of 348 m^2/s^2, and storm movement of 14 deg to the right at 79 percent of the 0-6 km mean wind (the mean wind in the layer from 0 to 6 km was 223 deg at 56 kt).

These values correlate well with the scatter diagram by Johns et al. (1993) which relates CAPE and helicity to the occurrence of strong tornadoes (Fig. 7).

4. WSR-88D Data

Reflectivity and velocity data from the Memphis WSR-88D proved very useful in identifying the severe thunderstorm that spawned the deadly Germantown tornado. (Times referred to below are the beginning times of the volume scans. The radar was being operated in mode VCP 11, indicating volume scans approximately five min in length.)

A squall line developed rapidly after 1800 UTC just ahead of the approaching surface trough. The storm that would produce the Germantown tornado intensified rapidly near Pine Bluff, Arkansas, in response to the erosion of the capping inversion. It was on the southern end of the squall line—a favored location for tornadic storms. The storm moved northeast with the mean flow and evolved into a high precipitation (HP) supercell. The 2100 UTC reflectivity data (see color plate, top figure) showed the HP supercell, with its characteristic kidney bean shape, moving into southwest Tennessee. The storm exhibited high reflectivities, with a broad area greater than 50 dBZ. The storm bulged eastward ahead of the squall line, allowing inflow to the storm to increase.

The table below shows information from the WSR-88D mesocyclone alphanumeric product. The table also gives estimates of rotational velocity of the storm that were computed manually, as well as the corresponding strength of the mesocyclone as obtained from the nomogram developed by the Operational Support Facility (OSF) at Norman, Oklahoma.

Time (Z)	Event	Base (K ft)	Top (K ft)	Azran Deg/nm	Height (K ft)	Diameter (Rad nm/ Az nm)	Rotational Velocity (KTS)	Shear (E^-3/sec)	Strength of Meso
2030	3D Cor	3.4	8.2	217/44	8.2	2.8 / 2.9	30	7	Weak
2035	Meso	3.0	15.3	215/40	7.5	3.9 / 3.0	30	9	Weak
2040	Meso	2.6	16.8	213/36	13.6	3.0 / 2.8	31	11	Weak
2045	Meso	2.4	14.9	210/33	9.1	5.0 / 2.9	36	10	Moderate
2050	Meso	2.2	15.9	206/32	5.4	6.1 / 3.2	n/a	14	n/a
2055	Meso	1.9	16.6	201/29	7.1	5.7 / 2.8	n/a	21	n/a
2100	Meso	1.7	17.7	195/26	6.4	5.4 / 2.5	45	16	Strong
2105	Meso	3.7	15.7	187/22	5.6	5.4 / 2.3	45	19	Strong
2110	n/a	n/a	n/a	n/a	n/a	n/a	45	n/a	Strong
2115	Meso	3.0	11.1	167/18	4.7	3.6 / 2.5	45	19	Strong
2120	TVS	2.7	10.3	155/16	7.1	3.4 / 2.0	50	49	Strong
2125	TVS	1.1	8.5	149/18	4.2	4.0 / 1.8	45	48	Strong
2130	Meso	1.0	2.9	134/17	1.0	2.0 / 2.3	45	57	Strong
2135	UncShr	3.0	3.0	121/18	3.0	1.6 / 1.9	45	14	Strong
2140	None						41		Moderate

Storm-relative velocities from the WSR-88D helped to identify the rotation associated with the mesocyclone. The mesocyclone algorithm first detected 3-D correlated shear with the storm at 2:30 p.m. (2030 UTC) when it was over northern Tunica County in Mississippi, about 38 miles southwest of Germantown. The WSR-88D detected a mesocyclone 5 min later, with a storm-relative rotational velocity of 30 kt. The supercell tracked northeast, and the mesocyclone intensified as rotational velocities increased. Figure 8 shows the track of the mesocyclone.

By 2100 UTC the mesocyclone had a rotational velocity of at least 45 kt and a depth of 16,000 ft (color plate), meeting the criteria for a strong mesocyclone.

It is important to note that storm-relative rotational velocities could not be computed at 2050 and 2055 UTC due to a problem with the WSR-88D data. It is possible the mesocyclone may have become strong prior to 2100 UTC. Subsequently, the rotational velocities peaked at or above 50 kt at the 2.4 deg elevation at 2120 UTC near the time the tornado touched down. The WSR-88D first detected a Tornadic Vortex Signature (TVS) at 2120, then again at 2125 UTC, after touchdown. The mesocyclone persisted for several more volume scans as it tracked into Fayette County, Tennessee, where sporadic damage was reported.

5. Warning Services

The severe weather on Sunday, November 27, was anticipated both by NSSFC (SELS) and by NWSFO Memphis forecasters as early as Friday night/Saturday morning. Forecasts mentioned possible severe thunderstorms, beginning with the 4:15 p.m. CST Saturday zone forecast package. A Special Weather Statement issued at 2:13 p.m. Saturday highlighted the potential for severe thunderstorms in west Tennessee on Sunday and urged residents to monitor later forecasts. A State Severe Weather Outlook issued early Sunday morning elaborated on the threat.

SELS placed west Tennessee in an area of slight risk for severe thunderstorms in their first Convective Outlook on Sunday morning; but upon examination of the 1200 UTC soundings, they upgraded the region to a high risk. A Tornado Watch was issued at 12:13 p.m. that included all of west Tennessee. The watch included enhanced wording that highlighted the threat of very damaging tornadoes.

Statements issued prior to the event mentioned that "thunderstorms are expected to develop and intensify rapidly, so plan now what you will do if severe weather strikes." Indeed, storms did develop rapidly as the cap eroded and the high levels of instability were released. While isolated severe storms affected the Memphis county warning area around noon, the most explosive development occurred between 2:30 and 3:30 p.m. CST.

Warnings were issued for several storms in the broken line of storms. The Germantown storm prompted a Severe Thunderstorm Warning at 3:04 p.m., with Severe Weather Statements following up on the storm's progress. At the time the Germantown tornado was developing (2:50-3:20 p.m.) there were severe storms in progress over a large part of the Memphis County warning area, from northwest Tennessee into north Mississippi. All warnings issued that

afternoon mentioned the possibility of tornadoes. A Tornado Warning was issued at 3:24 p.m. for the storm near Germantown.

6. Discussion

The WSR-88D proved to be an invaluable tool in the rapid detection of severe weather features, and it aided in the decisions that led to specific and timely warnings. Utilization of the WSR-88D was very labor-intensive during the event, however, especially when dealing with multiple severe storms in different parts of the county warning area. Procedures will be developed that will facilitate this as meteorologists become more familiar with the new radar.

Spotters were extremely helpful in obtaining ground-truth information during the event. The SKYWARN Amateur Radio Network was activated at 7:30 a.m. on Sunday, and amateur radio operators remained in the office until 9:00 p.m. There were no real-time visual sightings of the Germantown tornado, despite the fact that the tornado struck a heavily populated area in the middle of the afternoon. This was due in part to the tornado being associated with an HP supercell, with very heavy rain hindering the spotters' views. The first indications of the severity of the situation were reports from the Tennessee Highway Patrol of debris blocking a state highway in the area.

Finally, it is important to point out that the tornado occurred on a Sunday afternoon on Thanksgiving weekend. The three fatalities were all in one house, gathered together with about ten other family members for Thanksgiving dinner. Forecasters at NWSFO Memphis recognized the severe weather threat on Saturday and issued a special weather statement highlighting the severe weather risk for Sunday. Lessons learned from the Palm Sunday outbreak of March 1994 prompted the office to issue the special weather statement early, since public access to weather information may be limited on Sunday mornings.

Forecasters should attempt to learn from past events, such as the Palm Sunday outbreak or the Germantown tornado, and strive to improve not only their meteorological skills, but also techniques for providing warning and forecast services to the public. In order to recognize subtle tornado events, one should first be able to recognize the more obvious ones. Prior knowledge of environmental conditions, including shear and instability, is critical in the proper interpretation of WSR-88D products. Practice may not necessarily make perfect, but the lessons learned from post-analysis of severe weather episodes can certainly go a long way toward improving the accuracy and timeliness of future warnings and the quality of the services provided to the public.

Acknowledgements

The authors would like to thank Joseph Rogash (NSSFC) for his assistance in obtaining preliminary radar data, as well as surface and satellite data. Also, thanks to Gerald Rigdon, Richard Coleman, and John White (NWSFO Memphis) for their helpful review and valuable comments on the manuscript.

References

Gaffin, D., and R. Smith, 1995: Severe Weather Climatology for the NWSFO Memphis County Warning Area. *NOAA Tech. Memo. NWS SR-169.* 15 pp.

Hart, J.A., and J. Korotky, 1991: *The SHARP Workstation v 1.50.* A Skew-T/hodograph analysis and research program for the IBM and compatible PC. User's manual. NOAA/NWS Forecast Office, Charleston, WV.

Johns, R.H., and J.M. Davies and P.W. Leftwich, 1993: Some wind and instability parameters associated with strong and violent tornadoes, 2. Variations in the combinations of wind and instability parameters. *The Tornado: Its Structure, Dynamics, Prediction and Hazards.* Geophysical Monograph No. 79, American Geophysical Union, pp 583-590.

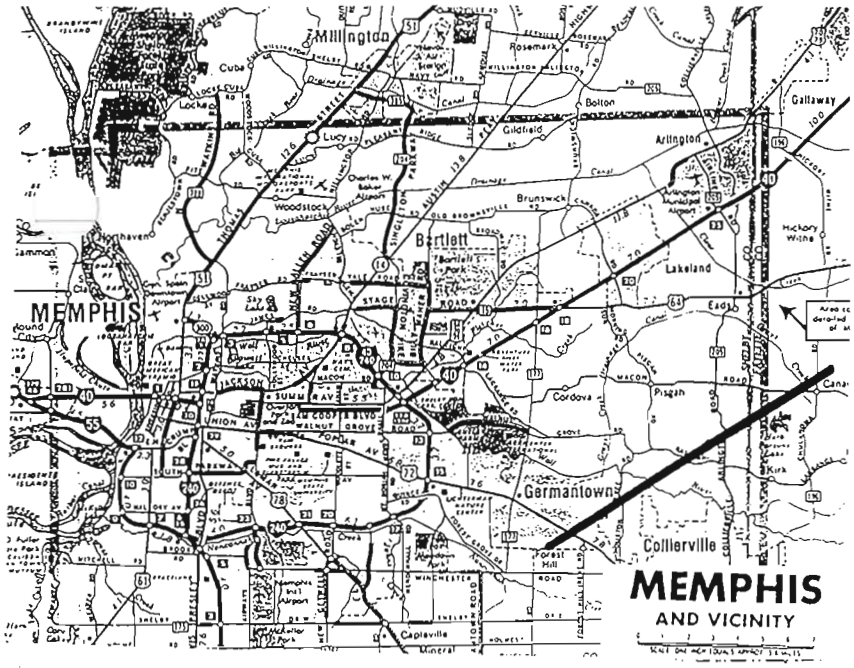

Figure 1. Approximate path of the Germantown tornado, November 27, 1994.

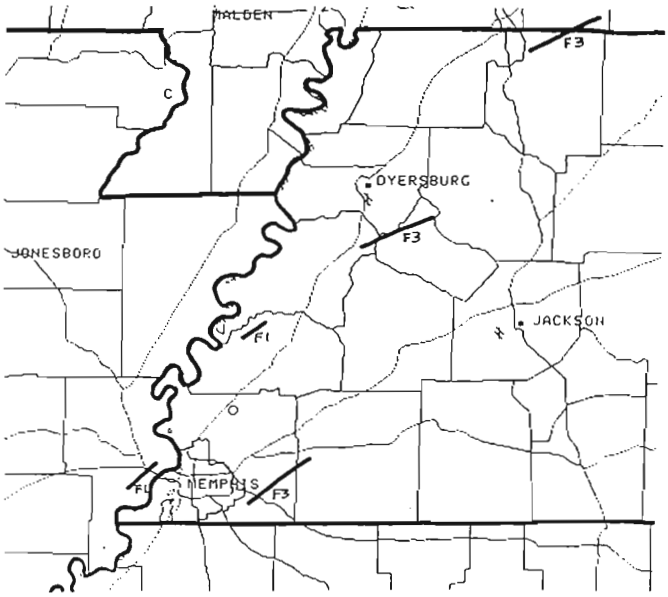

Figure 2. Paths and F-scale intensities of other mid-South tornadoes on November 27, 1994.

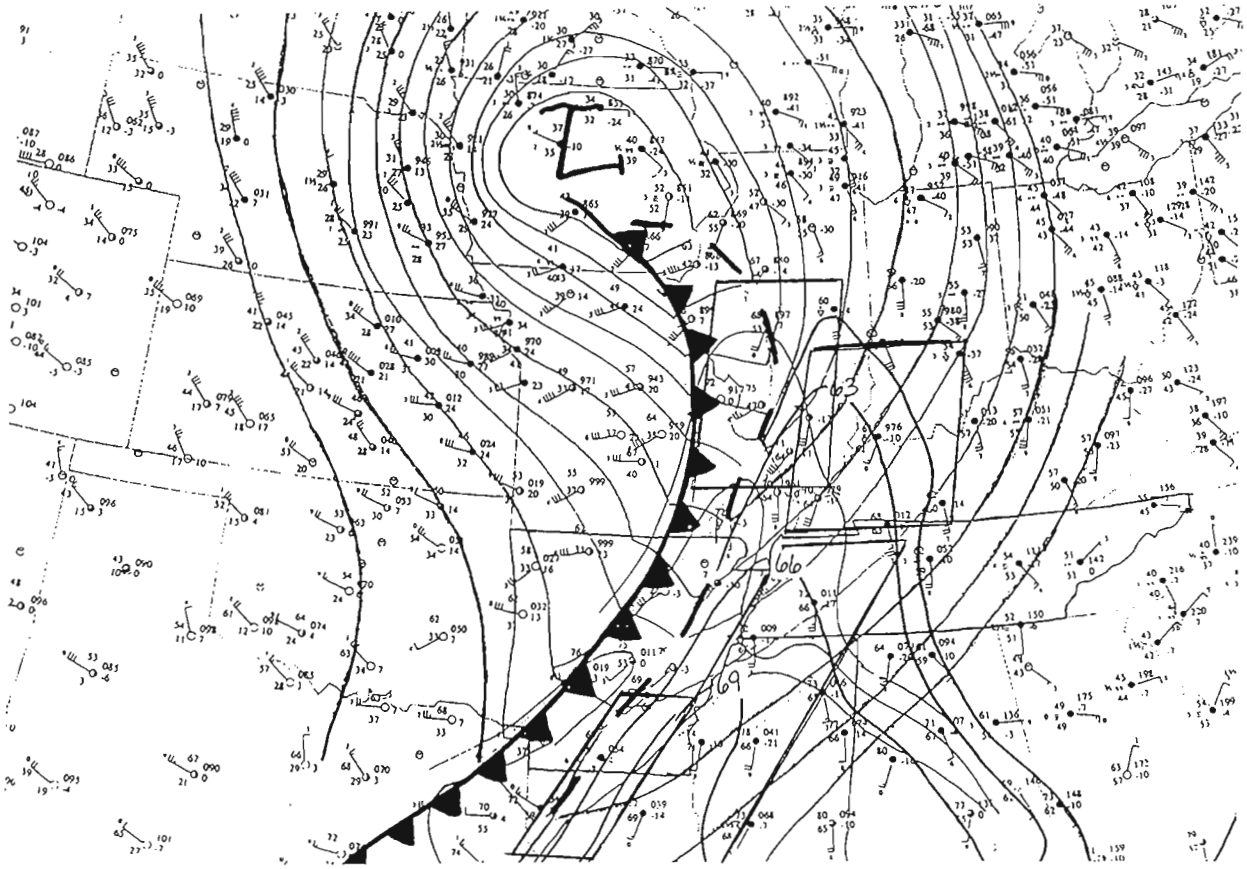

Figure 3. Surface analysis at 2100 UTC, November 27, 1994 (from NSSFC). Fronts, isobars and isodrosotherms shown, along with watch boxes in effect at the time.

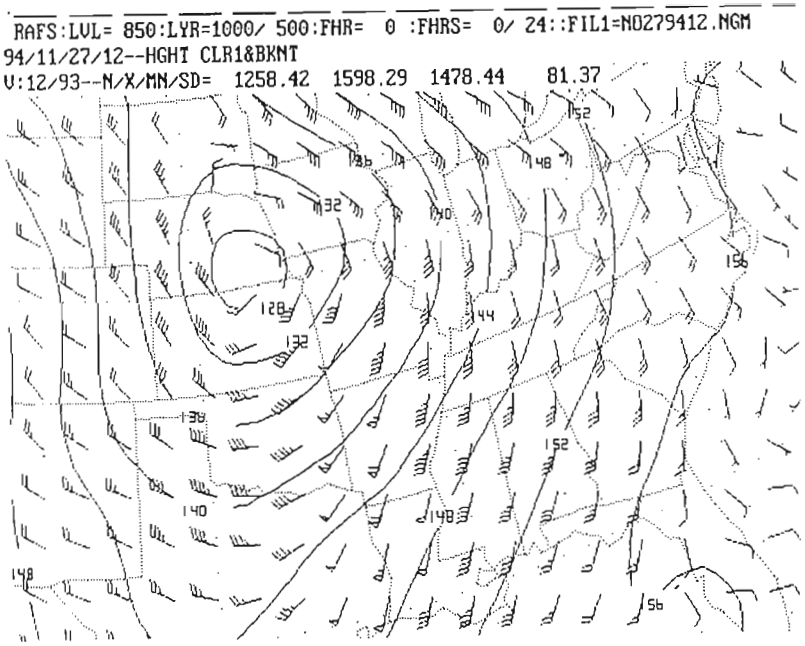

(a) heights (solid) and winds;

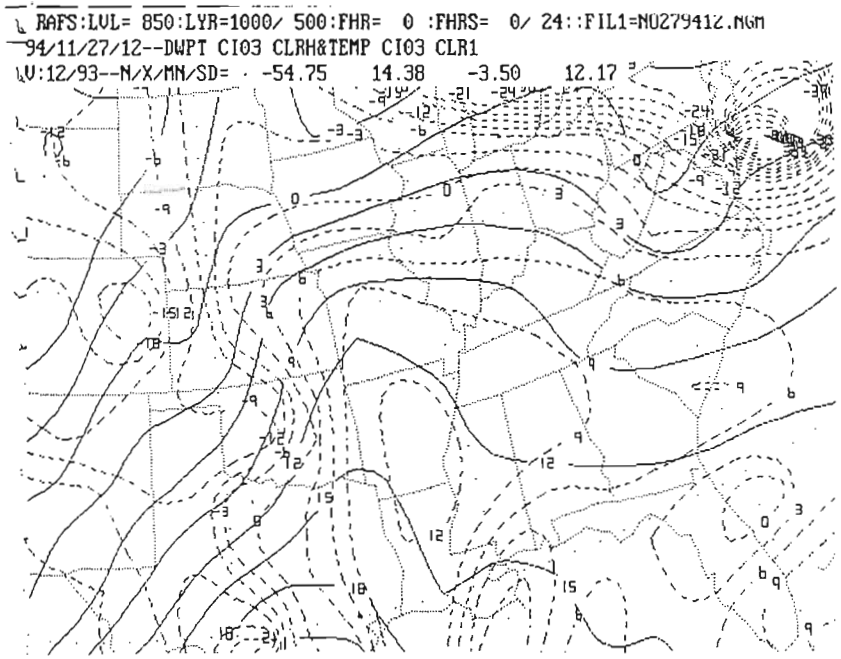

(b) temperature (solid) and dewpoint.

Figure 4. RAFS 850 mb analysis at 1200 UTC November 27, 1994.

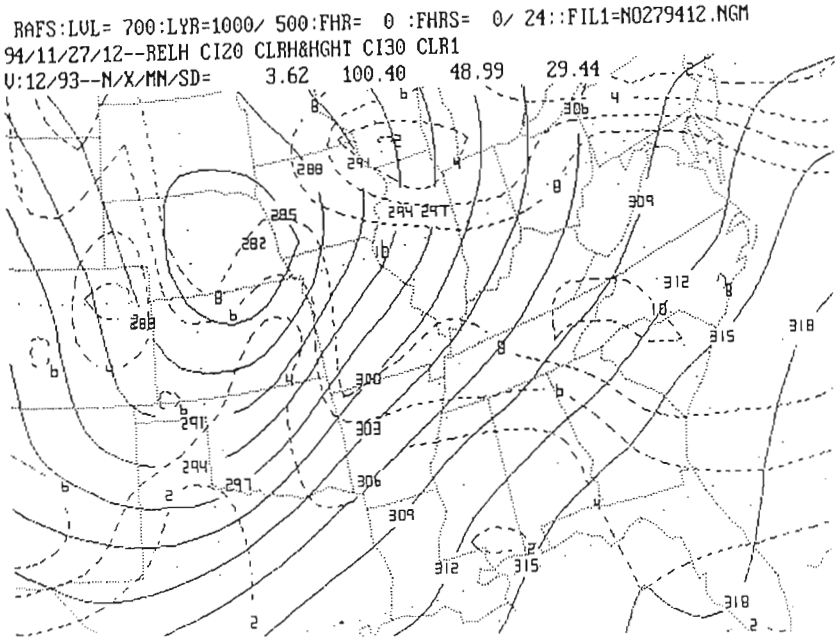

(a) 700 mb heights (solid) and relative humidity.

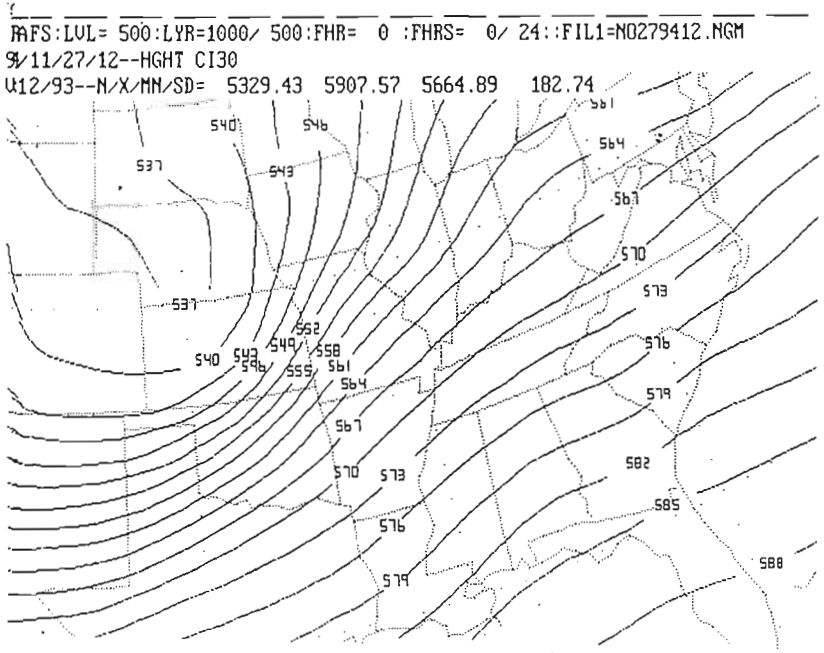

(b) 500 mb heights.

Figure 5. RAFS analyses at 1200 UTC November 27, 1994.

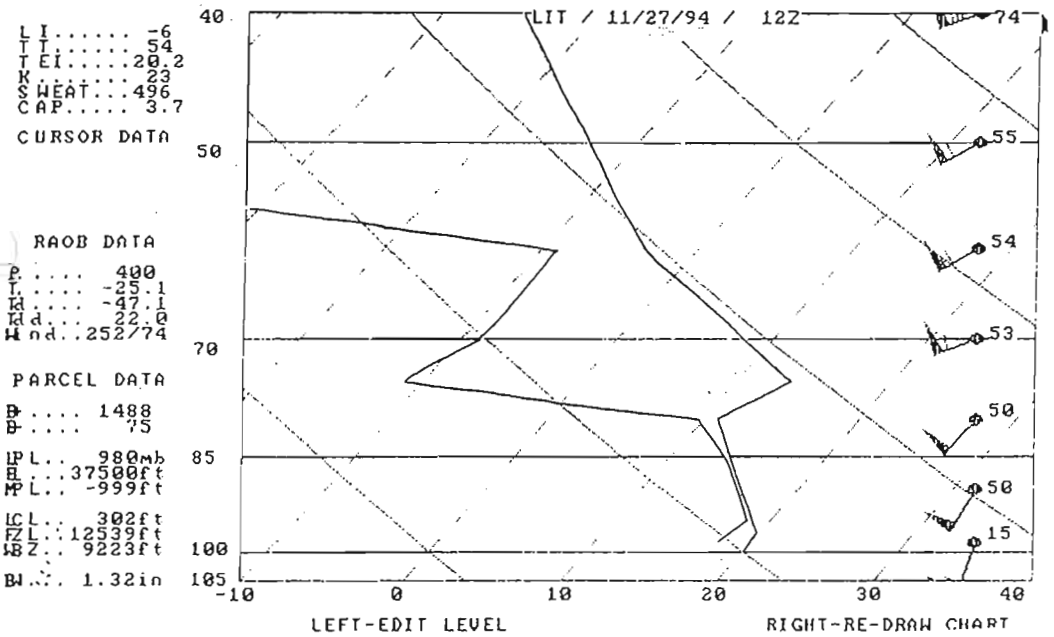

(a)

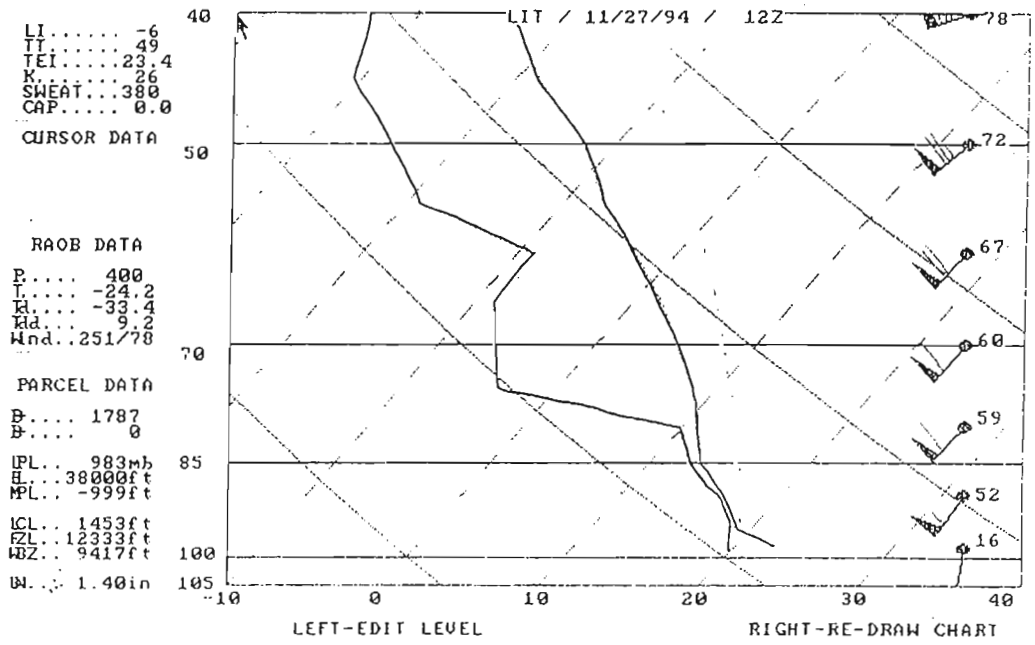

(b)

Figure 6.

Little Rock sounding at 1200 UTC November 27, 1994. (a) original sounding; (b) modified sounding (see text for details); (c) hodograph derived from modified sounding.

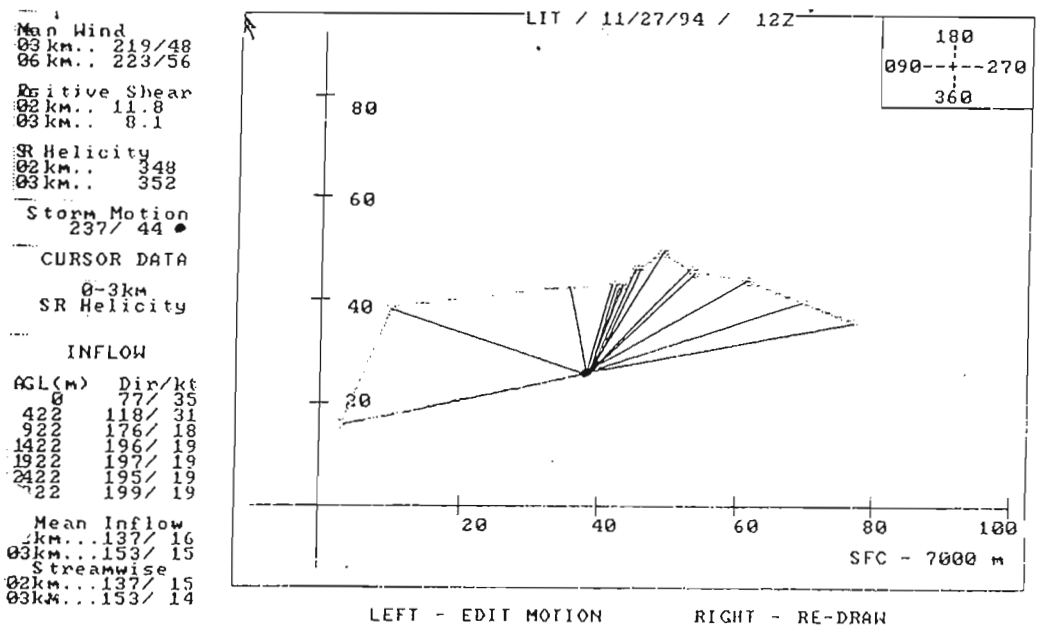

(c)

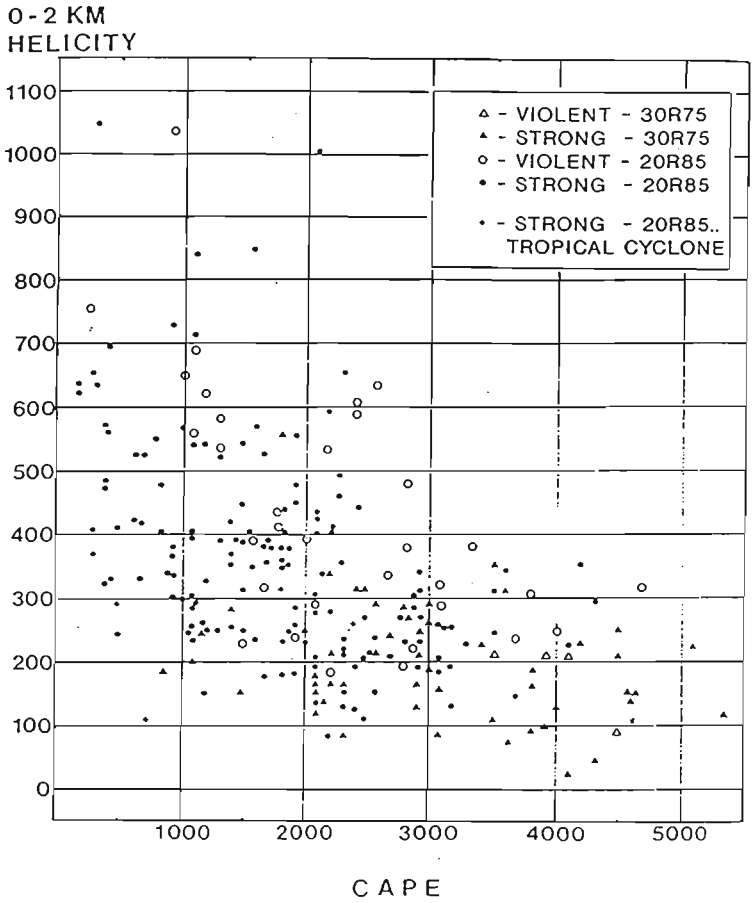

Figure 7. Scatter diagram showing relationship between CAPE and storm-relative helicity (from Johns, et al. 1993).

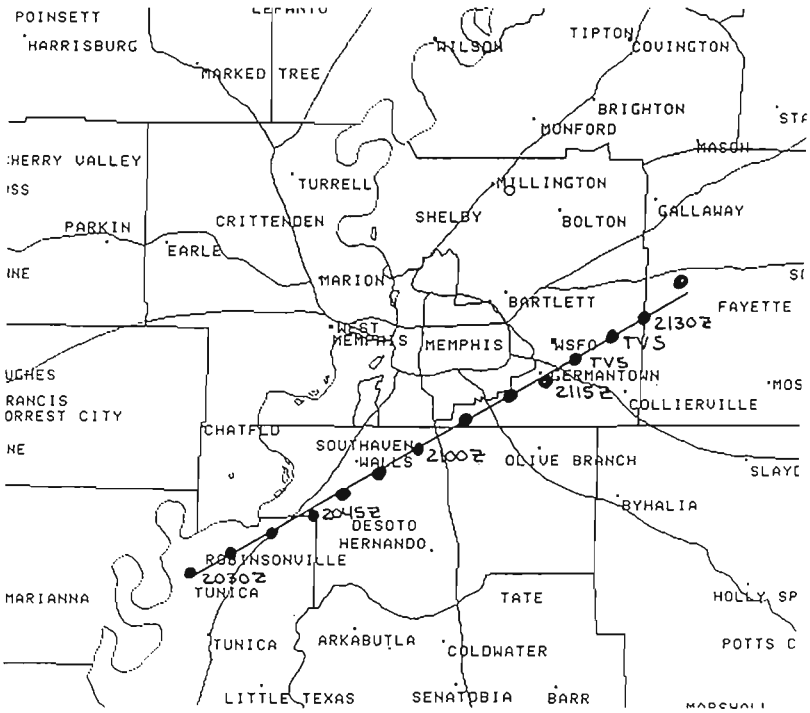

Figure 8. Track of mesocyclone that produced the Germantown tornado. Times refer to beginning of volume scans.

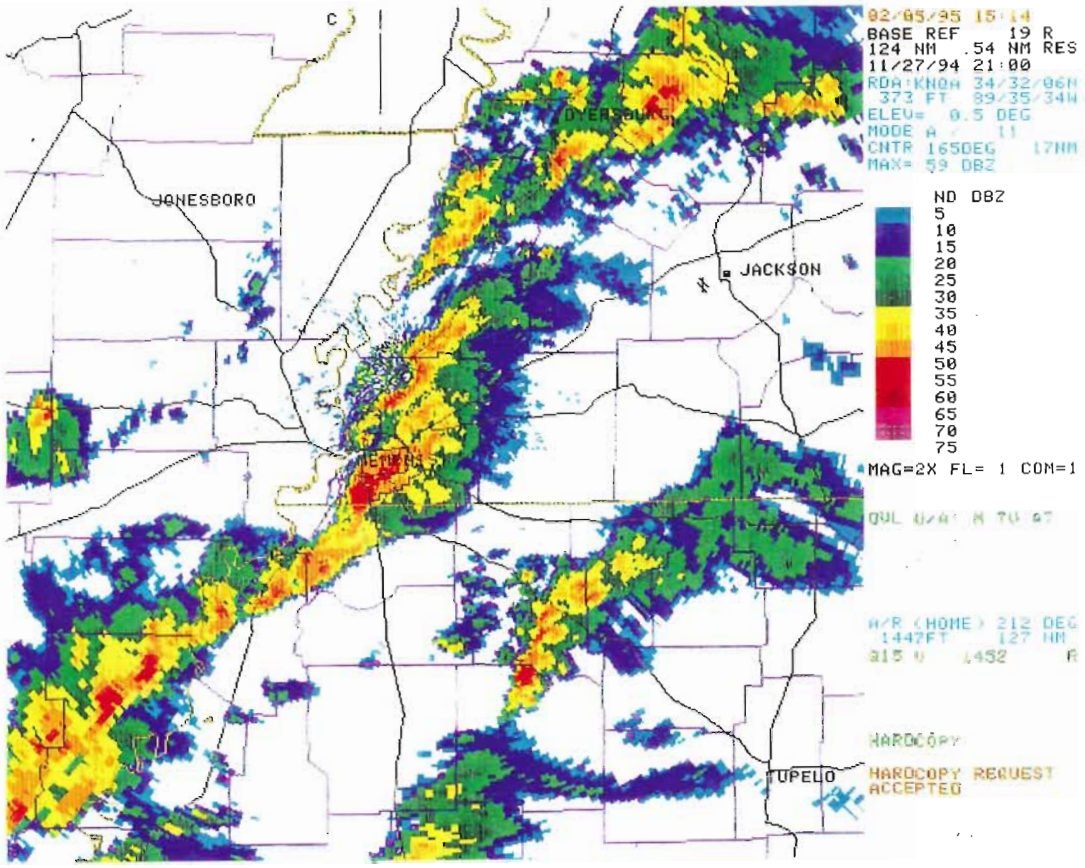

Color plate. Above: Base reflectivity at 2100 UTC November 27, 1994. Below: storm-relative velocity, same time as above, at selected elevation angles, as noted.

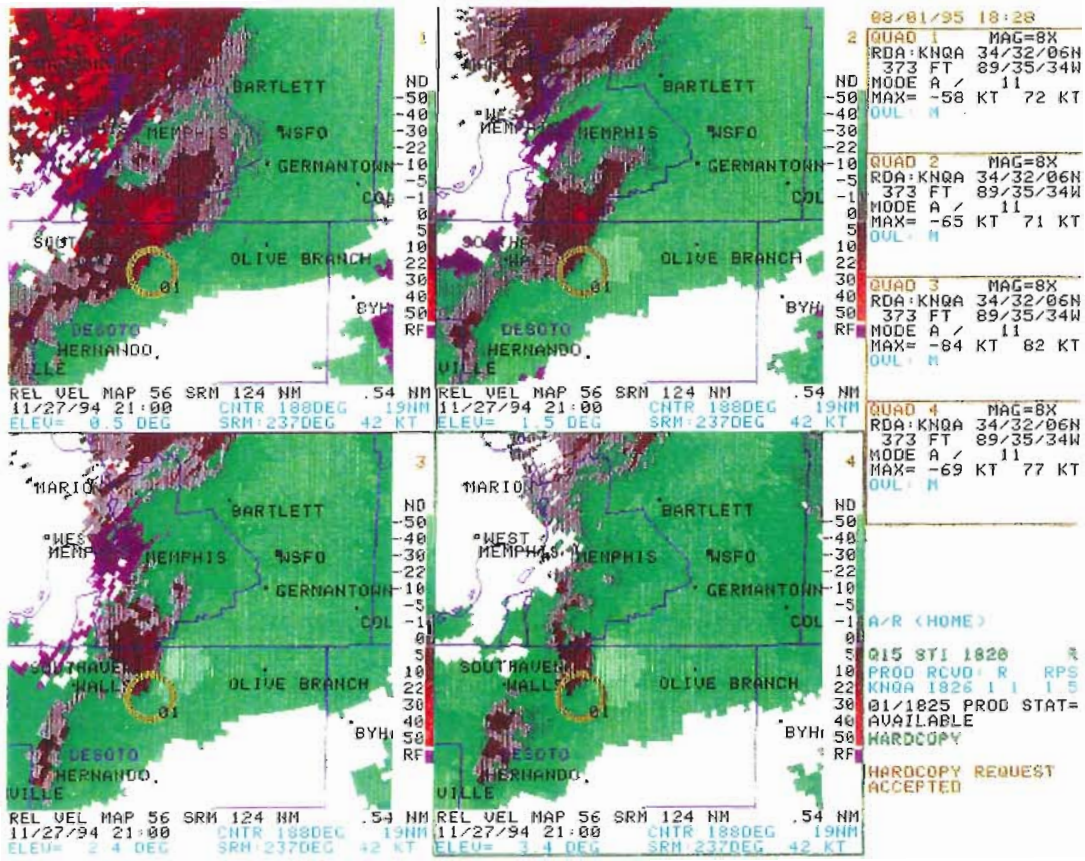

ON THE IMPORTANCE OF USING BASE SPECTRUM WIDTH DURING WIND EVENTS

Mark Richards and Tim Troutman
NWSO Nashville

Introduction

On April 11, 1995, a wind storm struck the middle Tennessee area. Damage to trees, power lines, and small structures was widespread; and further inspection revealed that the majority of the damage occurred from a 30-mi wide band of 50- to 70-kt winds that developed on the back edge of a precipitation area. One death resulted from the damaging wind as well in south central Kentucky. The area most affected in Tennessee is outlined in Fig. (a) in the accompanying color plate.

This study demonstrates why, along with WSR-88D base velocity data, the spectrum width products may also prove to be important in forecasting the onset of potentially damaging winds.

Synoptic Situation

Convection seemed to play a very small role in generating the damaging winds that occurred during this event. Deep low pressure was centered over southern Missouri with an associated cold front extending due south. High pressure just off the Eastern Seaboard set up a strong pressure gradient over middle Tennessee, thus providing 20- to 40-kt surface geostrophic winds (Fig. 1).

The Nashville sounding on April 11 at 1200 UTC (Fig. 2) showed the atmosphere to be marginally unstable. A modified version showed that further destabilization would be possible. Wind speeds from 30 kt at 1000 mb to near 55 kt at 700 mb were seen. Twelve hours later, the 0000 UTC sounding (Fig. 3) showed very similar winds.

Gridded model data from the 1200 UTC Eta and NGM model runs on April 11 showed that winds would increase by 1800 UTC. The NGM showed an increase from near 40 kt to near 50 kt at 850 mb, while the Eta showed the wind increasing to near 60 kt by 1800 UTC. Subsequently, the Eta model was found to have correlated better with the actual winds.

Around 1200 UTC on April 11, a large area of light to moderate rain (20-35 dBZ) began moving into middle Tennessee. This area moved across Nashville by 1800 UTC and moved on to the east around 2100 UTC. The band of damaging winds was evident on the immediate trailing edge of the precipitation area. A closer look at the synoptic pattern also revealed that along with the strong low-level jet, dry air was intruding into the back edge of the rain area. Evaporative cooling likely set up a nearly dry adiabatic lapse rate which further helped accelerate the descending air, thus aiding development of the damaging wind band.

Evaluating WSR-88D Products

The NWSO Nashville WSR-88D base reflectivity, base velocity, and storm-relative mean radial velocity products were initially used to determine the location and maximum wind speeds within the band. Base velocity (color plate, [a]) seemed to give the best results. Remembering, however, that only radial velocities (V_r) can be displayed, the equation $V_r = V \cos b$ must be applied to compute the true wind speeds (V), where b is the angle between the radial and the actual wind vector. Using these calculations, we estimated that true wind speeds ranged from about 55 kt at 3500 ft to about 105 kt at 7600 ft AGL. These velocities were computed from the mid-point values but rounded for sake of simplicity. A chart developed locally speeds up the process of calculating winds (see Fig. 4).

Figure (b) in the color plate shows the relationship of base reflectivity at 1423 UTC to the jet maximum, as indicated by the wind speeds determined above. A north/south cross section (not shown) that was taken at the precipitation/no precipitation edge indicated much higher reflectivity cores southwest of Nashville between Lexington and Waynesboro. This area was under the right entrance region of a mid-level jet maximum where rising motion is normally expected. Much lower reflectivity values were displayed northwest of Nashville between Waverly and Dover. This area was under the right exit region, where subsidence is expected. In later reflectivity products, the evidence became stronger as voids in the precipitation area began to develop.

After receiving numerous reports of 50- to 70-kt surface wind gusts and studying the 1423 UTC WSR-88D data, it was determined the most damaging winds were occurring almost on the immediate trailing edge of the precipitation area. If evaporative cooling was causing a descent of higher momentum air and the base spectrum width (color plate, [c]) showed a high variability in the wind flow, then it was thought possible the spectrum width product might indicate the higher momentum air as it neared or reached the surface. In this case, the high values of spectrum width correlated almost perfectly with the location of the damaging winds. An hour later, the 1525 UTC base spectrum width product (color plate, [d]) still correlated well with the area of damaging winds, and with the high wind warnings that were issued.

Discussion

In this case, the base spectrum width data were useful in locating the area of damaging winds. Does this mean that whenever we see high values of spectrum width we can expect wind damage? Not likely. Large values of spectrum width may indicate highly sheared environments, strong turbulence, eddies, jetlets, boundaries or gusts fronts; but smaller values may show the same thing. The velocity data from 1423 UTC (color plate, [a]) around Centerville, Tennessee (about 55 nm southwest of the RDA), indicate winds near 75 kt approximately 5800 ft above the surface. The corresponding 1423 UTC spectrum width values (color plate, [c]) at the same location were very low, however, even though sporadic damage did occur. The same velocity data near Paris, Tennessee (about 85 nm west of the RDA), showed wind speeds near 110 kt approximately 10,500 ft above the ground. The spectrum width data at this location revealed large values, and damage occurred there as well.

It is important to realize that the base spectrum width product reflects variability in the wind field. So why did damage occur in areas of low spectrum width values? Centerville is about 55 nm from the Nashville WSR-88D. At that distance, the sampling volume has a diameter of around 5600 ft. Paris is 85 nm from the radar, making the sampling volume around 9000 ft in diameter. Wind variability is likely to increase as the size of the sample volume increases. Although the values of spectrum width were relatively low at 55 nm, the velocity data indicated 75 kt winds around 5,800 ft, meaning that the majority of the wind flow in that 5600 ft sample volume was likely in the 75-kt range. With a jet that strong and so low in the atmosphere, the downdrafts associated with even weak convection (20-35 dBZ in this case) will likely be sufficient to bring higher momentum air to the surface, resulting in localized damage.

Conclusion

This case study using base spectrum width shows that during the April 11, 1995, wind event, values in the range of 12 kt or greater correlated quite accurately with widespread locations of reported wind damage. One could display spectrum width at any given time, even in clear weather, and likely find high values. However, if a low-level or mid-level jet exists across the area, there is an increased possibility that higher momentum air may descend to the surface, especially if convective downdrafts are present. Evaporational cooling makes this possibility even more likely. The base spectrum width product is definitely worth investigating in such synoptic situations. When utilized in conjunction with velocity products, spectrum width may help to accurately forecast the onset of high winds, which may ultimately lead to damage. In this case, the spectrum width product allowed 10- 15-min lead times in the issuance of high wind warnings across the Nashville county warning area.

We encourage more frequent use of this product in order to discover other possible operational applications. We have looked at two other cases where base spectrum width has given very good results with respect to the location of widespread wind damage. Up to this point, a common and distinct feature in all three cases has been the presence of a strong surface pressure gradient.

Acknowledgments

The authors thank Henry Steigerwaldt, Science and Operations Officer at NWSO Nashville, for his comments and suggestions on improving this manuscript. We also appreciate the comments and suggestions provided by Stacy Stewart, Meteorologist Instructor at the WSR-88D Operational Support Facility/Training Branch, Norman, Oklahoma.

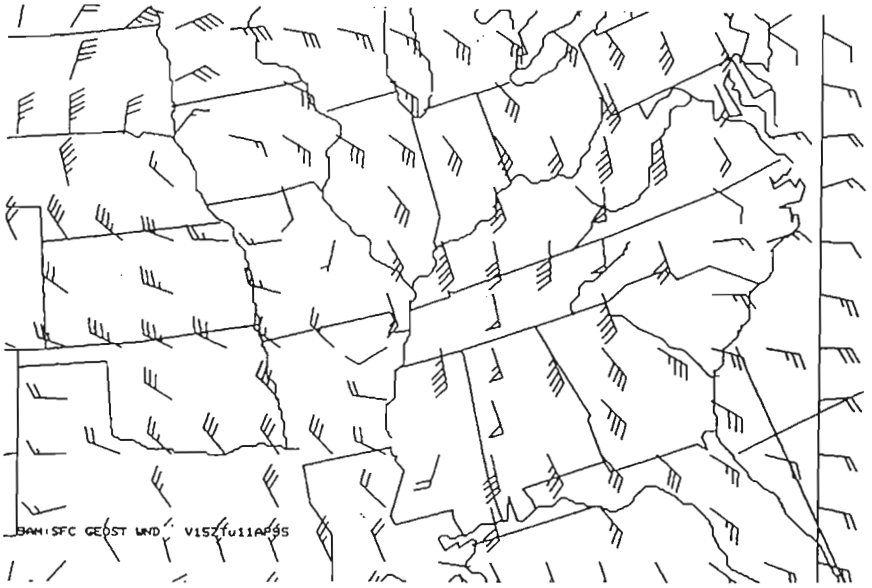

Figure 1 15 UTC Geostrophic Wind 04/11/95

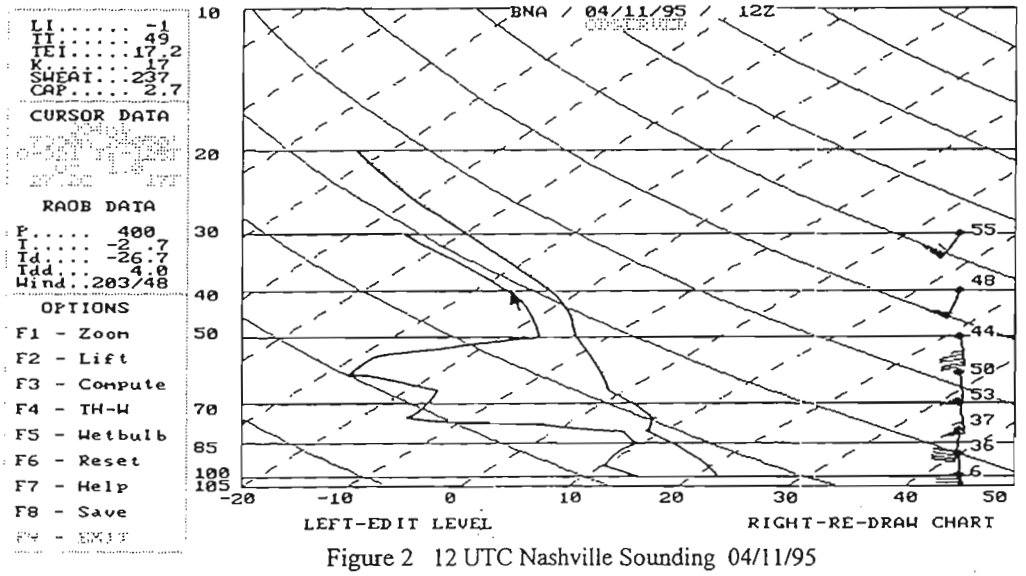

Figure 2 12 UTC Nashville Sounding 04/11/95

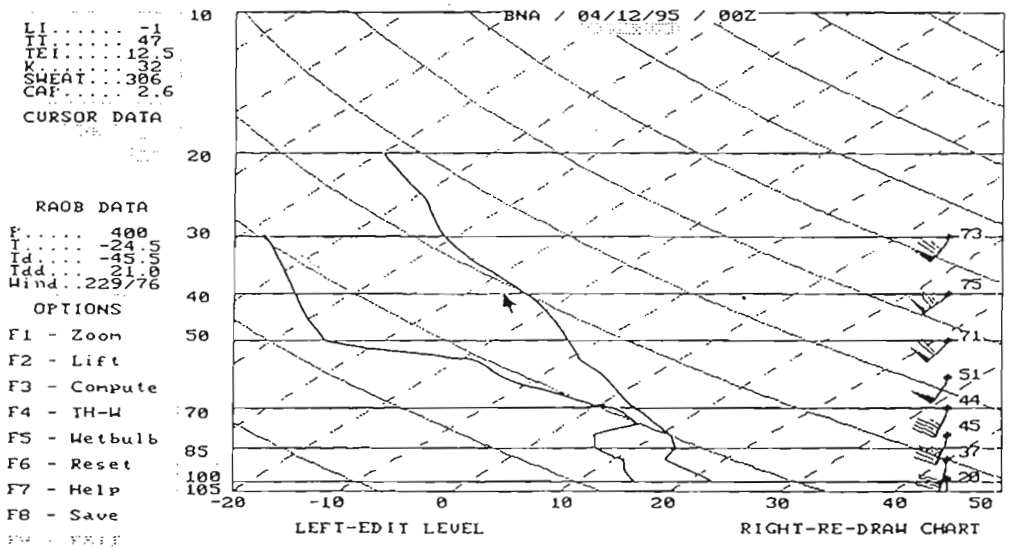

Figure 3 00 UTC Nashville Sounding 04/12/95

TRUE WIND VELOCITY

ANGLE OF WIND VECTOR TO RADIAL (DEGS)						
	80	86	132	179	248	328
	70	44	67	91	126	167
	60	30	46	62	86	114
	50	23	36	48	67	89
	40	20	30	40	56	74
	30	17	27	36	50	66
	20	16	24	33	46	61
	10	15	23	31	44	58
	0	15	23	31	43	57

SEVERE

WSR-88D BASE VELOCITY MID-RANGE VALUE (KTS)

EXAMPLE:

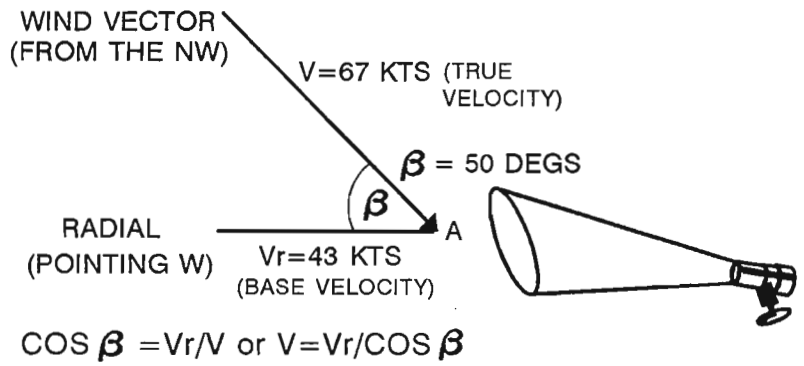

$\cos\beta = Vr/V$ or $V = Vr/\cos\beta$

UNLESS THE WIND VECTOR IS PARALLEL TO THE RADIAL AT POINT A, THE RADAR CAN ONLY DETERMINE PART OF THE TOTAL COMPONENT OF THE WIND VECTOR AT POINT A. THUS, A BASE VELOCITY VALUE OF 43 KTS IS IN REALITY 67 KTS.

Fig. 4

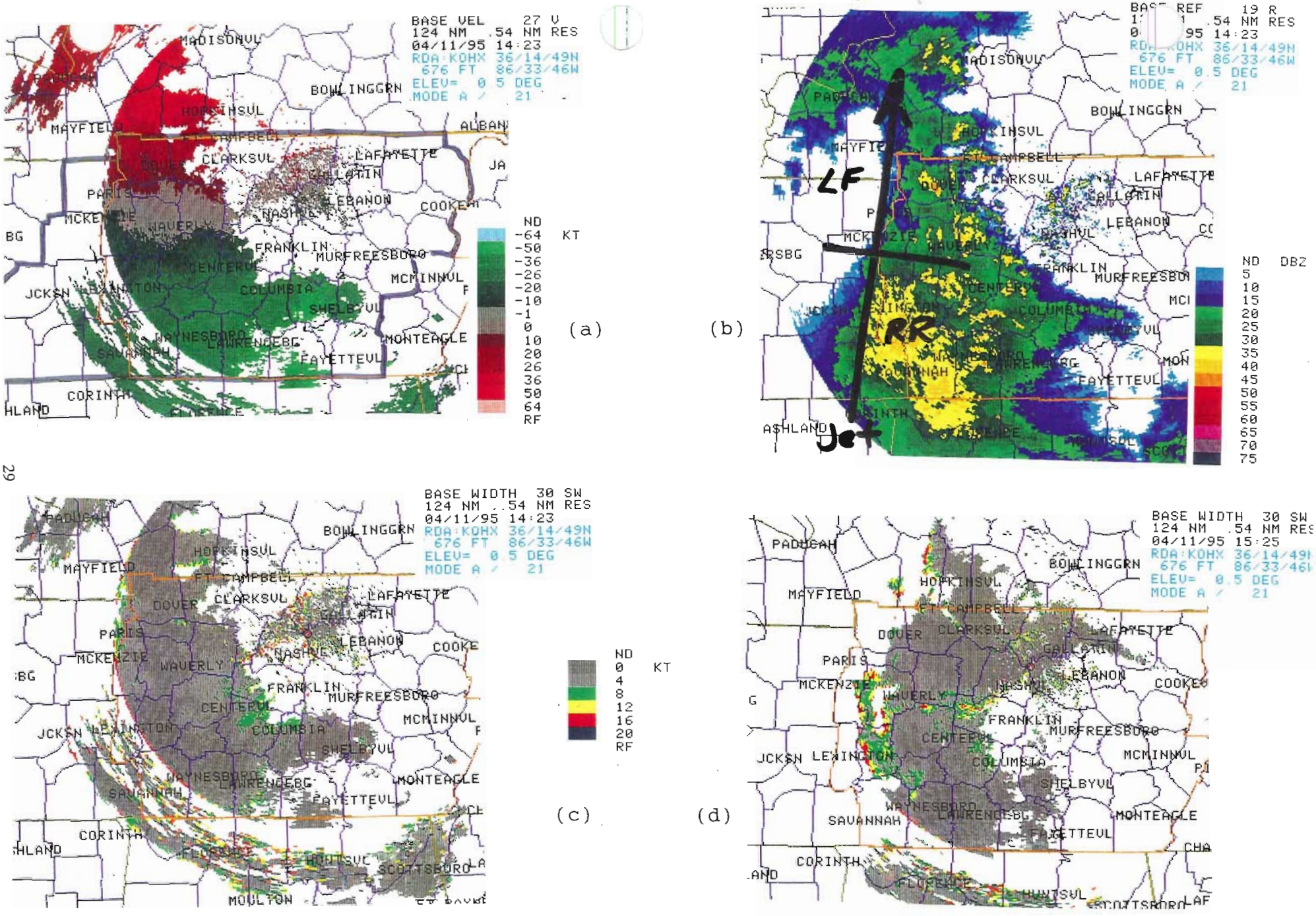

29

Color Plate. All products from NWSO Nashville WSR-88D, April 11, 1995. (a) 1423 UTC base velocity, area of damaging winds outlined; (b) 1423 UTC base reflectivity; (c) 1423 UTC base spectrum width; (d) 1525 UTC base spectrum width.

RECORD RAINFALL AT DAYTONA BEACH, FLORIDA, DURING TROPICAL STORM GORDON

Wayne Presnell and Jeff Borzilleri
WSO Daytona Beach, Florida

Introduction

During the late evening of November 15, 1994, and through the next 24 hr, 10.15 in of rain fell at the National Weather Service office in Daytona Beach, Florida, setting a record for 24-hr rainfall. This rainfall was associated with Tropical Storm Gordon as it moved from the southeastern Gulf of Mexico through central Florida. Preliminary estimates indicate that nearly $275 million in crops were lost in Florida due to flooding.

As with most tropical systems, extremely heavy rainfall can be expected over the area affected, especially in the northeast quadrant of the storm, which was where Daytona Beach was located in this case. However, the rain that fell between 0600 and 1000 UTC on the 16th exceeded that of a typical rainband associated with a hurricane (1.2 in/hr) as indicated by Anthes (1982). The rain gauge at the Daytona Beach NWS office recorded 5.20 inches in 4 hr. Investigation shows that the slow movement of the storm allowed two very intense rainbands to move very slowly across the Daytona Beach area, contributing to the record rainfall.

Data Sources

This study used surface observations and rain measurements from WSO Daytona Beach, WSR-88D radar products from the NWSO in Melbourne, and tropical discussions and advisories issued by the National Hurricane Center (NHC) in Miami.

Surface and radar observations and measurements extracted from rain gauge charts were examined to determine the period of most intense rainfall. This period was between 1 a.m. and 5 a.m. (0600 to 1000 UTC) on the 16th. Other periods of heavy rain occurred, but they were not as intense or prolonged. Tropical discussions and advisories from NHC indicated the position, movement, and strength of TS Gordon during the period of heaviest rain. This information indicated that Gordon moved very slowly and did not strengthen during this period. Gordon's movement through central Florida allowed Daytona Beach to remain in the northeast quadrant of the storm during the heavy rainfall episodes.

Synoptic Setting

At 0000 UTC on Tuesday, November 16, TS Gordon was located 100 nm south of Sarasota, Florida, moving northwest at 7 kt with a central pressure of 998 mb (Fig. 1). Gordon displayed a closed circulation through 500 mb and was vertically stacked. Isotachs at 300 mb showed wind speeds less than 10 kt over most of Florida and the Gulf of Mexico. A large area of high pressure was centered over the west-central Atlantic and extended westward to the East Coast of the United States.

By 0600 UTC, about the time the heaviest rain began at Daytona Beach, Gordon had moved to about 115 nm south of Sarasota. The storm was drifting north-northeastward with a central pressure of 997 mb. NMC models showed a vertical velocity maximum at 250 mb directly over Daytona Beach. The ridge of high pressure remained in the same location. By 1200 UTC the storm had moved to just offshore of Fort Meyers with little change in intensity. The ridge had moved slightly to the northeast, and a strong short-wave trough was located over the central United States.

Discussion

a. WSR-88D Radar observations

Figures 2a-d from the NWSO Melbourne WSR-88D show the composite reflectivities at 0600, 0900, and 1200 UTC on the 16th, and the estimated storm total precipitation between 1300 UTC on the 14th and 1200 UTC on the 16th. This covers the most intense period of rainfall in the Daytona Beach area (0600 to 1000 UTC on the 16th), during which the rain gauge at the Daytona Beach NWS office recorded 5.20 in.

At 0600 UTC on the 16th, an intense band of rain was located from just west of Daytona Beach to approximately 35 nm offshore from Melbourne (Fig. 2a). The maximum intensity within this band was 50-55 dBZ about 15 nm east-southeast of Daytona Beach. The cells within this band were moving slowly from the east-southeast and the band was drifting northward. Another area of very heavy rain (50-55 dBZ) extended from the southern portion of Cape Canaveral, southward to between Melbourne and Vero Beach.

By 0900 UTC (Fig. 2b) the second band of extremely heavy rain had moved north and was located over Daytona Beach. The WSO measured 3.92 in during the previous 3 hr. The heavy rain band extended from Daytona Beach southeast to about 20 mi offshore from Cape Canaveral. The cells continued to move slowly from the east-southeast while the band was moving slowly northward.

Figure 2c shows that by 1200 UTC less intense rain was over the Daytona Beach area (35-40 dBZ). The total rainfall at the NWS office between 0600 and 1200 UTC was 5.67 in. Extremely heavy rain was still occurring 10 to 20 nm east-southeast of Daytona Beach, but the rainband was moving north a little faster than before. Cells were still moving from the east-southeast; but by the time the heaviest cells moved onshore, they were north of Daytona Beach. The table below summarizes the period of heaviest rain at the NWS office.

Figure 2d shows the only storm-total precipitation product available to the authors from the Melbourne WSR-88D. It covers the period between 1300 UTC on the 14th and 1200 UTC on the 16th, during which time the radar indicated a total of 4 to 5 inches in the Daytona Beach area. For the same time period, the total rainfall at the NWS office in Daytona Beach was 7.43 in, indicating an underestimate on the part of the radar precipitation algorithm. It should be noted, however, that the WSR-88D is approximately 75 nm from Daytona Beach, at which

Time Period UTC	Total Accumulated Rainfall in Inches
0600 (16th) - 0900 (16th)	3.92
0600 (16th) - 1000 (16th)	5.20
0600 (16th) - 1200 (16th)	5.67
2000 (15th) - 2000 (16th)	10.15

range the center of the radar beam (at its lowest elevation) is at about 6000 ft elevation, which probably accounts for some of the underestimation.

Note, however, that Fig. 2d shows the heaviest precipitation from TS Gordon occurred in a narrow band between Daytona Beach and about 30 nm offshore from Cape Canaveral. The largest computed rainfall was nearly 10 in approximately 20 nm southeast of Daytona Beach (about 60 nm from Melbourne). Most of this rainfall was also associated with rainbands from Gordon. If the observed/algorithm ratio from Daytona Beach is used to scale this offshore amount, then it is not unlikely that a total of more than 15 in is closer to the truth.

b. Slow Movement of Gordon

Perhaps the most important factor in the extremely heavy rainfall was the slow movement of TS Gordon. At 0600 UTC on the 16th, when the period of heaviest rain began, Gordon was moving very slowly over the southeastern Gulf of Mexico. By 1200 UTC, Gordon was still offshore from Fort Meyers and was moving northeast at 8 kt. Gordon did not strengthen during this time as the central pressure remained at 997 mb.

The storm moved northeast across central Florida in response to the strong short wave over the central United States. Gordon's northeast movement was most likely impeded by the ridge over the Atlantic, however. Outer convective rainbands associated with tropical storms are typically stationary or move very slowly when there is strong high pressure to the northeast (Anthes 1982).

TS Gordon's slow movement allowed the rainbands to move very slowly over the Daytona Beach area, creating large rainfall totals. After 1200 UTC, Gordon was moving to the northeast at 5-10 kt, taking the heaviest rainfall north of Daytona Beach. After 1200 UTC, and for the remainder of the day, heavy rain occurred periodically near Daytona Beach; but the intensity and duration did not match that of the previously discussed rainbands. It is interesting to note that no thunder or lightning was observed at the NWS office during TS Gordon.

Conclusions

The extremely heavy rains (10.15 in) that fell at the NWS office in Daytona Beach, Florida, during the evening of November 15 through the afternoon of November 16, 1994, set a record

for rainfall at the office in a 24-hr period. The rainfall was associated with TS Gordon as it moved from the southeastern Gulf of Mexico across central Florida.

The most intense rain occurred between 0600 and 1000 UTC (1 a.m. to 5 a.m.) on the 16th. It is typical for extremely heavy rainfall associated with tropical systems to occur at night in the northeast quadrant of the storm. Indeed, composite reflectivity from the WSR-88D in Melbourne, Florida, indicated that two intense rainbands moved over the Daytona Beach area between 0600 and 1200 UTC on the 16th. The slow movement of TS Gordon allowed these outer rainbands to move very slowly over the Daytona Beach area, increasing the rainfall significantly and aiding in creating record 24-hr rains at the NWS office. Indeed, it is likely that even heavier rains occurred a short distance away, luckily over the Atlantic.

Slowly moving rainbands from Gordon clearly were associated with the heavy rains in this case, but it is possible that other factors may have contributed to why the bands produced such intense rain. Other factors might include mesoscale features associated with kinematic flow into the bands, moisture convergence, and enhanced vertical motion. An investigation of these factors is beyond the scope of this brief study. In any event, examining WSR-88D products and closely tracking the movement and position of rainbands will provide important guidance for determining areas at risk for heavy rains associated with tropical systems over Florida.

Acknowledgment

The authors would like to thank Mr. Dave Sharp, Science and Operations Officer at NWSO Melbourne, for his help in obtaining the WSR-88D products used in this study.

Reference

Anthes, R.A., 1982. Tropical Cyclones, Their Evolution, Structure, and Effects. *Meteorological Monographs, 19, 41.* Amer. Met. Soc., Boston, MA. pp 37-46.

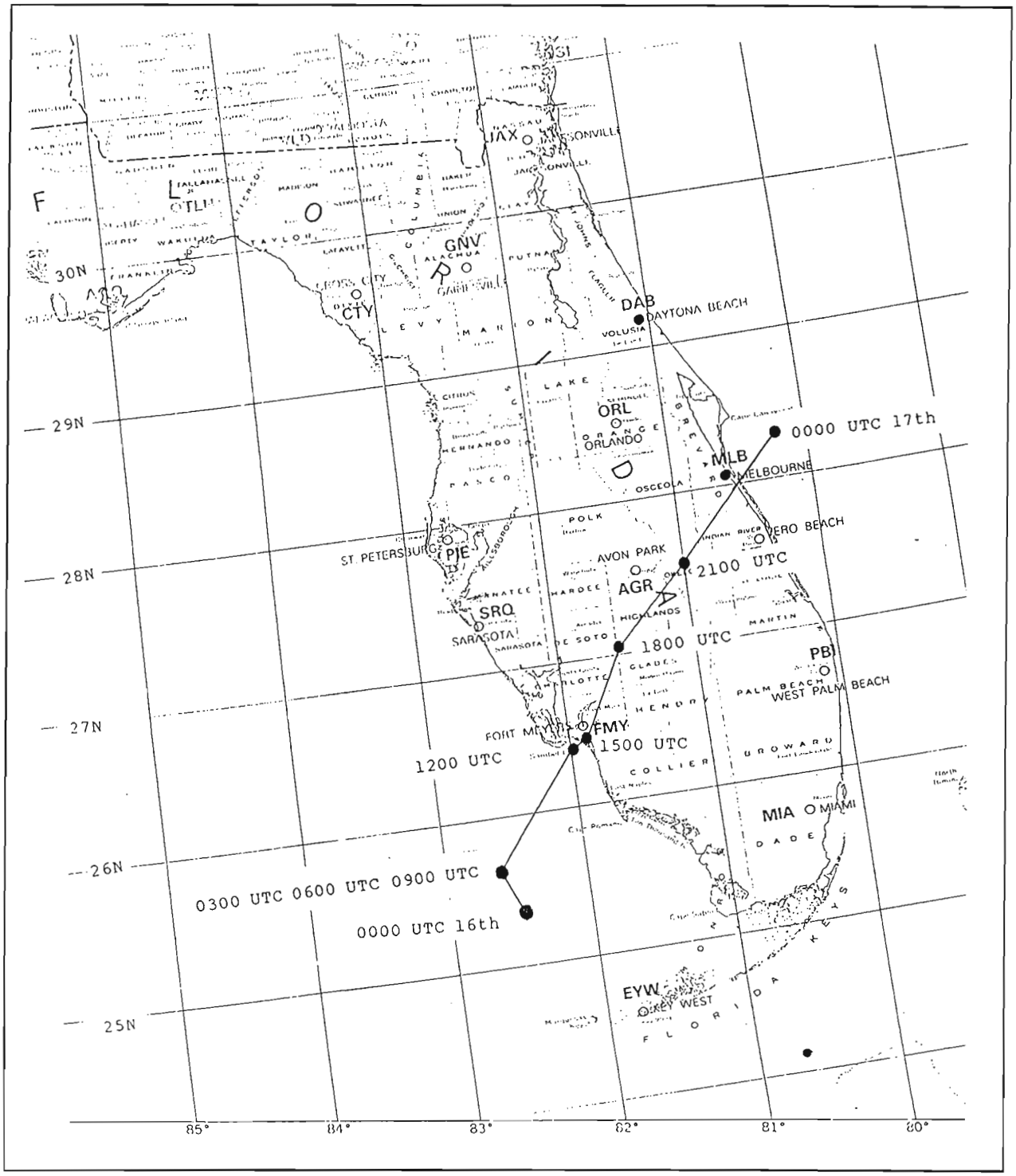

Fig. 1. Three hourly positions of Tropical Storm Gordon, 0000 UTC November 16 to 0000 UTC November 17, 1994.

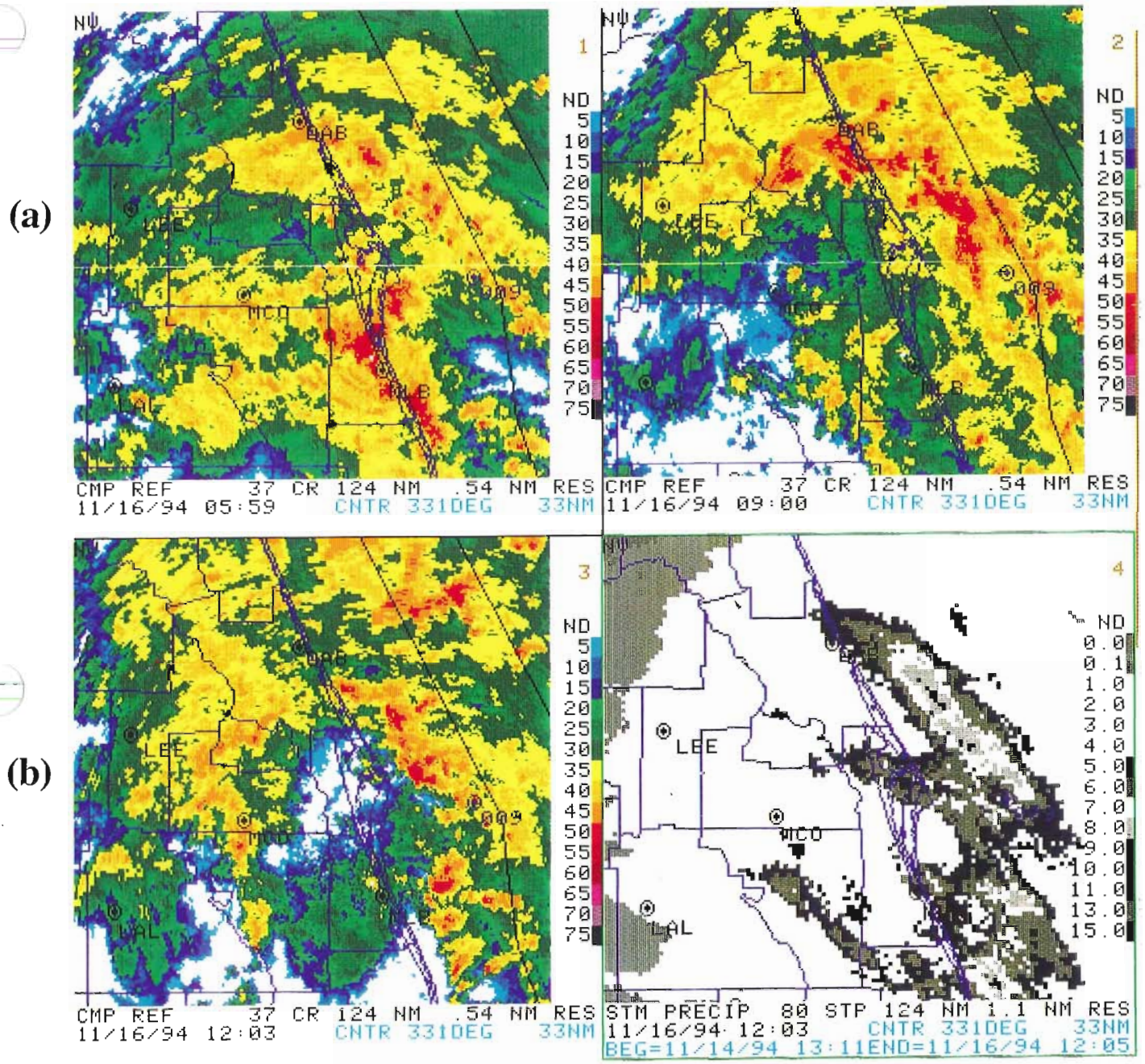

Fig. 2. Composite reflectivities from the WSR-88D at NWSO Melbourne during Tropical Storm Gordon: (a) 0600 UTC, (b) 0900 UTC, and (c) 1200 UTC November 16, 1994. Fig. (d) is the storm total precipitation as estimated by the WSR-88D.